Journal of Mammalian Evolution (2023) 30:819–844
https://doi.org/10.1007/s10914-023-09673-5

RESEARCH

Petrosal morphology of the Early Cretaceous triconodontid *Astroconodon* from the Cloverly Formation (Montana, USA)

Simone Hoffmann[1] · **E. Christopher Kirk**[2,3] · **Timothy B. Rowe**[3] · **Richard L. Cifelli**[4]

Accepted: 8 June 2023 / Published online: 5 August 2023

Abstract

Although several well-preserved crania are known for the Mesozoic Eutriconodonta, three-dimensional reconstructions of the character-rich inner ear and basicranial region based on high-resolution computed tomography scans have previously only been published for the Late Jurassic *Priacodon*. Here we present a description of the petrosal and inner ear morphology of a triconodontid eutriconodontan from the Lower Cretaceous Cloverly Formation, which we provisionally assign to *Astroconodon*. The bony labyrinth of *Astroconodon* is plesiomorphic for mammaliaforms in lacking a primary osseous lamina, cribriform plate, and osseous cochlear ganglion canal. However, as in *Priacodon* and the zhangheotheriid *Origolestes*, *Astroconodon* has a secondary osseous lamina base that extends nearly the complete length of the cochlear canal. The cochlear canal is straighter in *Astroconodon* and other eutriconodontans compared to several basal mammaliaform clades (e.g., morganucodontans, docodontans), that exhibit varying degrees of cochlear canal curvature. The pars cochlearis of the petrosal was well vascularized in *Astroconodon*, exhibiting a network of venous canals that crossed the cochlea transversely on its ventral and dorsal aspects. Of particular note are several canals that passed along the base of the secondary osseous lamina. As in *Priacodon* and *Origolestes*, those canals do not show the extensive connections to the cochlear labyrinth as seen in the basal mammaliaforms *Morganucodon* and *Borealestes*. The inner ear of *Astroconodon* thus highlights the complex history of the mammaliaform cochlear canal, in which different clades appear to follow independent evolutionary trajectories and various key morphological features (e.g., cochlear canal length, curvature, vascularization and osseous supports for the basilar membrane) exhibit considerable homoplasy.

Keywords Mammal · Eutriconodonta · Inner ear · Mesozoic

✉ Simone Hoffmann
simone.hoffmann@nyit.edu

E. Christopher Kirk
eckirk@austin.utexas.edu

Timothy B. Rowe
rowe@mail.utexas.edu

Richard L. Cifelli
rlc@ou.edu

[1] Department of Anatomy, College of Osteopathic Medicine, New York Institute of Technology, Old Westbury, NY 11568, USA

[2] Department of Anthropology, University of Texas at Austin, Austin, TX 78712, USA

[3] Department of Geological Sciences, University of Texas at Austin, Austin, TX 78712, USA

[4] Department of Vertebrate Paleontology, Sam Noble Oklahoma Museum of Natural History, University of Oklahoma, Norman, OK 73072, USA

Introduction

Triconodontidae comprise a family of Jurassic–Cretaceous mammaliaforms nested within Eutriconodonta (e.g., Kielan-Jaworowska et al. 2004; Gaetano and Rougier 2011; Martin et al. 2015; Rougier et al. 2021). The group was first established by Marsh (1887) to include the Late Jurassic *Priacodon* and Early Cretaceous *Triconodon* based on the shared presence of three nearly equal-sized, mesiodistally aligned cusps on their molars. Simpson (1928, 1929) provided the first modern characterization of Triconodontidae, and added *Trioracodon* to the family, based on species from the Late Jurassic of North America and the earliest Cretaceous of the United Kingdom. Patterson (1951) and Fox (1969, 1976) assigned two additional genera from the Cretaceous to the family: *Alticonodon* (Santonian, Canada) and *Astroconodon* (Aptian–Albian, U.S.A.). A phylogenetic definition of Triconodontidae was

first established by Rougier et al. (1996: p. 3) as "the group including the last common ancestor plus descendants of the five genera included in Triconodontidae by Jenkins and Crompton (1979): *Alticonodon*, *Astroconodon*, *Priacodon*, *Triconodon*, and *Trioracodon*." Additionally, several newly named taxa have been incorporated into the family, including *Arundelconodon* (Aptian, U.S.A. – Cifelli et al. 1999), *Corviconodon* (Aptian–Albian, U.S.A. – Cifelli et al. 1998), *Meiconodon* (Aptian–Albian, China – Kusuhashi et al. 2009), and *Jugulator* (Albian–Cenomanian, U.S.A. – Cifelli and Madsen 1998). More recent phylogenetic analyses by Gaetano and Rougier (2011) and Rougier et al. (2021) have also added *Ichthyoconodon* from the Late Cretaceous of Morocco, *Argentoconodon* from the Early-Middle Jurassic of Argentina, and *Volaticotherium* from the ?Middle-Late Jurassic of China to Triconodontidae, but see Martin et al. (2015), Meng et al. (2006) and Mao et al. (2020) for an alternative placement of *Volaticotherium* and *Argentoconodon* outside of Triconodontidae. Additional Mesozoic taxa have been assigned to Triconodontidae but have not yet been included in phylogenetic analyses (e.g., an unnamed triconodontid from the Middle Jurassic of Kyrgyzstan – Martin and Averianov 2010; *Eotriconodon* from the Middle Jurassic of U.K. – Butler and Sigogneau-Russell 2016).

If *Argentoconodon* is a member of Triconodontidae, then the clade is known from all continents except Australia and Antarctica and spans almost 100 million years, from the Early/Middle Jurassic to the Late Cretaceous. Despite this large geographic and chronological range, articulated and complete cranial or postcranial material is relatively rare for Triconodontidae. Most triconodontid genera are known only from isolated teeth and fragmentary or disarticulated gnathic or cranial remains. This general dearth of more complete triconodontid specimens is in strong contrast to other eutriconodontans. Gobiconodontidae are known from several complete and articulated postcranial skeletons and well-preserved skulls (e.g., Jenkins and Schaff 1988; Li et al. 2001; Wang et al. 2001; Li et al. 2003; Hu et al. 2005; Hu 2006; Martin et al. 2015), and the unassigned eutriconodontans *Liaoconodon*, *Yanoconodon*, and *Jeholodens* are likewise known from nearly complete skeletons (Ji et al. 1999; Luo et al. 2007; Meng et al. 2011).

The three specimens (Museum of Comparative Zoology [MCZ] 19969, 19973, 19974) that are the focus of this study consist of cranial and postcranial material from the Lower Cretaceous Cloverly Formation of Montana. Such well-preserved and complete material is particularly rare for North American triconodontids. The specimens were collected in 1974–1975 by Farish A. Jenkins, Jr. and colleagues, and have been frequently referenced in the literature as the 'Cloverly triconodont', 'Cloverly Formation tricondontid' or 'Early Cretaceous triconodont' (e.g., Clemens et al. 1979; Jenkins and Crompton 1979; Wible 1991; Crompton and Luo 1993; Wible and Hopson 1993; Rougier et al. 1996; Cifelli et al. 1998). The specimens considered here were first mentioned by Jenkins and Crompton (1979), who reported 20 dental specimens of an unnamed triconodontid, ranging from fragmentary jaws to complete skulls, some with associated postcranial remains. In the same volume, Clemens et al. (1979: p. 30) also referred to the triconodontid fossils from the Cloverly Formation, noting that "it is an understatement to say that the scientific potential of these finds is extraordinary."

Following those initial references, the basicranial anatomy of the Cloverly triconodontid has been figured and partially described by Crompton and colleagues. Crompton and Sun (1985: fig. 7A) presented a reconstruction in ventral view, likely based on MCZ 19973. A more detailed description and reconstruction of the basicranium based on MCZ 19969 and MCZ 19973 was provided by Crompton and Luo (1993). Both reconstructions have been referenced by various authors, including Wible (1991), Lucas and Luo (1993), and Wible and Hopson (1993). Rougier et al. (1996) included the 'Cloverly triconodonts' in their phylogenetic analysis and comparison of the petrosal morphology of *Priacodon*. However, Rougier et al. (1996) left the family assignment of the 'Cloverly triconodonts' open, given that they were recovered as sister to an unresolved clade containing *Priacodon*, *Trioracodon*, and *Triconodon* in their phylogenetic analysis. Rougier et al. (1996) noted that whether the 'Cloverly triconodonts' should be included in Triconodontidae depends on the relationship not only with the triconodontids included in their phylogenetic analysis (*Priacodon*, *Trioracodon*, *Triconodon*), but also with the other two genera that define Triconodontidae: *Alticonodon* and *Astroconodon*. Both of these taxa were only known from dental remains and were therefore not included in the analysis of basicranial characters conducted by Rougier et al. (1996). More clarity on the relationship of the 'Cloverly triconodontid' was provided by Cifelli et al. (1998), who first mentioned a strong similarity to *Astroconodon denisoni* and supported a placement within Triconodontidae. We agree with the preliminary taxonomic assessment of Cifelli et al. (1998) and will accordingly here refer to the 'Cloverly triconodontid' as *Astroconodon* sp. Whether the fossils belong to *A. denisoni* or a new species of *Astroconodon* will be the topic of future analyses. In this paper we explore the character-rich basicranial anatomy of *Astroconodon*, with a particular focus on the inner ear and associated neurovascular structures.

Materials and methods

Specimens and preservation

The three specimens were collected in the Lower Cretaceous Cloverly Formation Unit V by field parties from the Museum of Comparative Zoology led by F. A. Jenkins, Jr.,

and C. R. Schaff in 1974–1975. The locality was discovered by Arnold D. Lewis and William Amaral, and has yielded eutriconodontan crania, mandibles, and postcranial material in concretionary nodules. A map of the locality can be found in Jenkins and Schaff (1988: fig. 2) labeled "Harvard triconodontid site". The description of the complete cranial and postcranial material, including systematic paleontology, diagnosis, geological setting, and preservation is currently in progress and will be published elsewhere. Here we will summarize only those aspects of preservation relevant to interpret the anatomy of the basicranial region.

The specimens were found in dense calcareous nodules that were recovered through a combination of quarrying and screen washing, and exposed through manual preparation. The calcareous nodules are similar to septarian nodules in many respects, including indications that postmortem burial was rapid (Astin 1986). Sediment overloading compressed the specimens to varying degrees, and it also produced tensile stress fields that induced extensive networks of anastomosing fractures throughout the bones. These fracture networks were then infilled by a dense cement that is probably a secondary precipitate of barite ($BaSO_4$) forming as an extracellular polymeric substance from biofilms living on the internal and external surfaces of the bones and inside the fractures (Martinez-Ruiz et al. 2018). Iron oxides and iron sulfides can also be precipitated by a postmortem microbiome living on and inside bones (Brown et al. 1999), but in this case the color and high density suggest the infill is primarily barite or some other barium compound. To the naked eye, the infill is nearly colorless, with only a slight blue-gray tint. On many surfaces, it is difficult to distinguish from the bone it intruded, in part because many of the intruding veins are quite thin, and those veins that extended beyond the bone surfaces into the surrounding nodular matrix were mechanically prepared away to the level of the bone surfaces.

In addition to infilling the network of cracks produced by taphonomic process, the barite also infilled the natural cavities within the petrosal (e.g., the bony labyrinth and neurovascular channels). The infill is far denser than the fossilized bone, which is particularly visible in the micro computed tomography (μCT) scans. The barite infilling the bony labyrinth and neurovascular channels in the petrosal appear in bright white grayscale values in the μCT scans. The density difference between the bone and infilling barite is so high that the bone appears in nearly the same range of grayscale values as the surrounding air.

Computed tomography and imaging

The specimens were μCT scanned at the University of Texas High-Resolution X-ray Computed Tomography Facility (UTCT) in 1999, 2002, 2015 and 2021. The abundance of barite infill in these fossils precluded most radiographic investigations for 20 years, until advances in technology permitted resolution of internal anatomy. The first attempt to μCT scan one of the skulls (MCZ 19974) in 1999 was largely defeated by the dense barite infill casting 'shadows' over the bone. Following an instrument upgrade in 2002, UTCT attempted to scan the skull of MCZ 19973, but once again the barite infill cast 'shadows' that severely compromised efforts to visualize internal skeletal anatomy. The data were not entirely uninformative, but imaging software and segmenting procedures in use at the time were unsuitable for generating publication-quality imagery. Subsequent UTCT upgrades to a new North Star Imaging (NSI) scanner, including a detector with greater sensitivity and resolution, and the capability of helical scanning, together with advances in imaging software, finally enabled the highly informative μCT datasets used here. Scans of the basicrania of MCZ 19973 and 19974 were generated in 2015, and in 2021 all three skulls (MCZ 19969, 19973, 19974) were scanned in their entireties. We used the 2015 high-resolution scans of the basicranial region for the reconstructions of the inner ear of MCZ 19974 and MCZ 19973, and the 2021 full skull scan for MCZ 19969. The petrosal images are based on the entire scan of the skulls from 2021, as the image quality was slightly better and was less impacted by high disparity in density between bone and infilling barite. Individual scan parameters for the key scans used in this analysis are listed below per specimen.

MCZ 19969 – 2021: NSI scanner, Fein Focus High Power source, 210 kV, 0.24 mA, brass filter, isometric voxel size 29.6 μm, 1871 total slices.

MCZ 19973 – 2015: NSI scanner, Fein Focus High Power source, 215 kV, 0.17 mA, aluminum filter, isometric voxel size 10.9 μm, 899 total slices. 2021: NSI scanner, Fein Focus High Power source, 210 kV, 0.24 mA, brass filter, isometric voxel size 12.9 μm, 3369 total slices.

MCZ 19974 – 2015: NSI scanner, Fein Focus High Power source, 215 kV, 0.13 mA, aluminum filter, isometric voxel size 11 μm, 1089 total slices. 2021: NSI scanner, Fein Focus High Power source, 210 kV, 0.24 mA, brass filter, isometric voxel size 13.4 μm, 3281 total slices.

TIFF stacks were imported into Amira 2020 (FEI ThermoFisher Scientific) for segmentation. 'Isosurface' and 'Volume Rendering', as well as labeling individual voxels in the Label Field Editor and extracting polygon surface files of labeled materials were used to render surface files. Label fields were smoothed using the 'grow label field in 3D' and then 'smooth 3D label field' option. Images of the endocast were taken in Amira using the 'Snapshot' tool. Surfaces files were displayed in Amira using the following 'Surface View' options: 'Specular' off, 'Opaque,' 'Both Faces,' and either 'Vertex normal' or 'Triangle normal.'

Measurements

All measurements were taken digitally in Amira using the '3D measurement tool'. Cochlear length was measured along the abneural curvature from the center of the fenestra vestibuli to the apex of the cochlear canal. Other inner ear measurements follow Schultz et al. (2017).

Institutional abbreviations

LACM, Los Angeles County Museum, Los Angeles; MCZ, Museum of Comparative Zoology, Harvard University, Cambridge; NHM, The Natural History Museum (formerly BM(NH)), London; OMNH, Oklahoma Museum of Natural History, Norman; PIN, Borissiak Paleontological Institute of the Russian Academy of Sciences, Moscow.

Description

Petrosal

One of the most prominent features of the petrosal in ventral view is the long and slender, 'fingerlike' promontorium (Fig. 1). The promontorium is only gently rounded, uninflated, and has a smooth surface that lacks distinct crests or grooves for neurovascular structures. At the posterior end of the promontorium are two large openings that are separated by the crista interfenestralis. The medial opening, the perilymphatic foramen, faces posteriorly and is almost circular (Table 1). A deep groove for the perilymphatic duct passes from the perilymphatic foramen medially toward the jugular notch. The groove is best seen on the right side of MCZ 19973 (Online Resource 1: Fig. S1a) and the left side of MCZ 19969 (Online Resource 1: Fig. S1c). The groove appears to be deeper in MCZ 19969 and shallower in MCZ 19974 (Online Resource 1), although this might be a preservational artifact rather than intraspecific morphological variation. The medial margin of the petrosal is incomplete in MCZ 19974 and it is possible that the part of the petrosal that contained the perilymphatic duct is not fully preserved. There do not appear to be any bony lappets covering the perilymphatic groove in MCZ 19973 or MZC 19969 and there is no evidence that the perilymphatic duct was partially or fully enclosed in bone in any of the specimens. *Astroconodon* thus retains the plesiomorphic condition for mammaliaforms in exhibiting an open perilymphatic groove and a perilymphatic foramen (Rougier and Wible 2006). The perilymphatic duct was not enclosed in bone and a cochlear aqueduct was not developed.

Posterior to the perilymphatic foramen and medial to the crista interfenestralis is a deep recess that is reminiscent of the recessus scalae tympani for the perilymphatic sac in *Ornithorhynchus*. The perilymphatic foramen and recess sit in a jugular fossa that also encompasses the jugular foramen. The medial border of the jugular fossa and jugular foramen is formed by the exoccipital, which is not preserved or is displaced in the three specimens. As such, the sizes of the jugular fossa and jugular foramen are unclear. Based on the preserved jugular notch in MCZ 19973 the jugular foramen was at least subequal in size compared to the perilymphatic foramen. Immediately anterior to the perilymphatic groove, along the medial border of the petrosal, is an opening for the inferior petrosal sinus

Table 1 Measurements of inner ear in *Astroconodon* sp. All measurements in mm. Cochlear canal length measured from center of fenestra vestibuli to apex of cochlear canal. Dorsoventral height and mediolateral width of cochlear canal measured at mid-length of canal. *ASC* anterior semicircular canal, *LSC* lateral semicircular canal, *PSC* posterior semicircular canal

	MCZ 19973 Right	MCZ 19973 Left	MCZ 19974 Right	MZC 19974 Left	MCZ 19969 Right	MCZ 19969 Left
Cranial length	43	43	–	–	–	–
Cochlear canal length	3.6	–	4.0	4.1	–	–
Cochlear canal height	1.0	1.0	1.0	1.1	–	–
Cochlear canal width	1.1	1.1	1.1	1.1	–	–
Fenestra vestibuli axes	0.9 x 0.5	–	1.1 x 0.7	–	–	–
Perilymphatic foramen axes	–	–	0.9 x 0.9	–	–	–
ASC height	1.7	–	1.8	–	1.7	2.1
ASC width	1.3	–	1.5	–	1.5	1.6
PSC height	2.4	–	2.6	–	2.8	–
PSC width	2.0	–	1.8	–	2.0	–
LSC height	1.5	–	1.7	1.6	1.8	1.9
LSC width	1.4	–	1.5	1.3	1.4	1.4

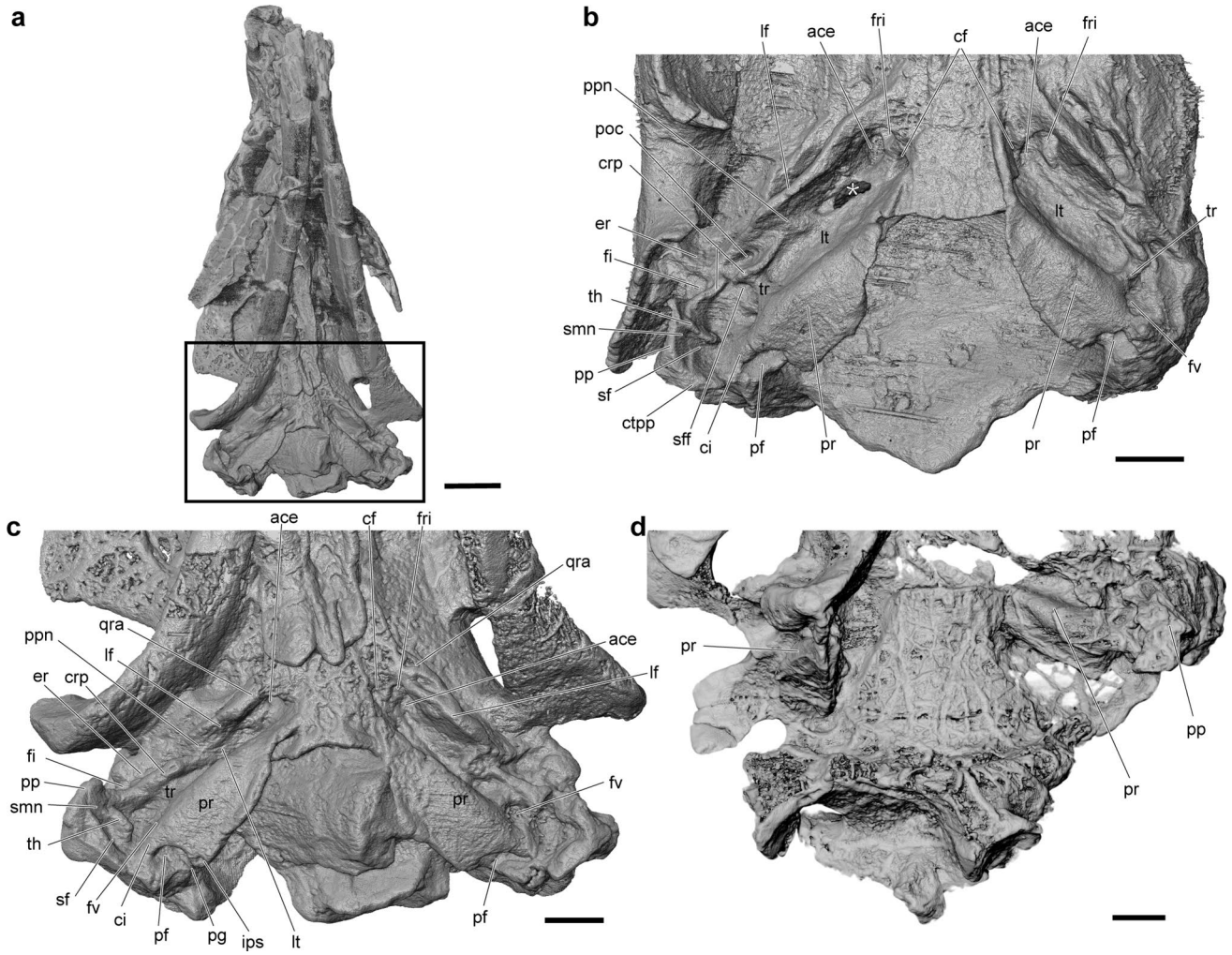

Fig. 1 Rendering of 3D virtual model of basicranial regions of *Astroconodon* sp. based on µCT data in ventral view. **a**. MCZ 19973 overview of cranium, area outlined with black rectangle is shown enlarged in **b**. **c**. MCZ 19974 and **d**. MCZ 19969. Asterisk in **b** indicates part of lateral trough that is broken in MCZ 19973. Abbreviations: **ace**, anterior opening of cavum epiptericum; **cf**, carotid foramen; **ci**, crista interfenestralis; **crp**, crista parotica; **ctpp**, caudal tympanica process of the petrosal; **er**, epitympanic recess; **fi**, fossa incudis; **fri**, foramen for inferior ramus of stapedial artery and post-trigeminal vein; **fv**, fenestra vestibuli; **ips**, inferior petrosal sinus; **lf**, lateral flange; **lt**, lateral trough; **pe**, petrosal; **pf**, perilymphatic foramen; **pg**, perilymphatic groove; **pp**, paroccipital process; **ppn**, pterygoparoccipital notch; **pr**, promontorium; **poc**, tympanic opening of prootic canal; **qra**, quadrate ramus of alisphenoid; **sf**, stapedial fossa; **sff**, secondary facial foramen; **smn**, stylomastoid notch; **tr**, transverse ridge; **th**, tympanohyal. Scale in **a** equals 5 mm, scale in **b–d** equals 2 mm

(Figs. 1c and 2a, d). The inferior petrosal sinus continues as a canal within the petrosal, passing anteriorly along the medial border of the cochlear canal (Fig. 3).

The opening lateral to the crista interfenestralis is the fenestra vestibuli for the footplate of the stapes. The fenestra vestibuli faces ventrolaterally and is oval-shaped, with a longer anteroposterior axis and a shorter dorsoventral axis (Table 1). The crista interfenestralis, between the fenestra vestibuli and perilymphatic foramen, extends from the promontorium to the base of the paroccipital process. The crista interfenestralis is a tall and horizontal ridge of bone that is continuous with the ventral surface of the promontorium (Fig. 1b, c).

The paroccipital process is large in *Astroconodon* and extends well past the ventral surface of the promontorium. It is best preserved on the right side of MCZ 19973 and 19974 (Fig. 1b, c). Part of the posterior paroccipital process is missing from the right side of MCZ 19974 but the curvature of the posterior paroccipital process is preserved on the left side. The paroccipital process is roughly triangular in ventral view (Fig. 1b, c), with a rounded corner that points posterolaterally. The paroccipital process is bifurcated with the posterior aspect extending posteromedially toward the crista interfenestralis (the thickened edge of which is the caudal tympanic process of the petrosal; Fig. 1b) and the anterior

aspect extending anteromedially (the anterior extension of which is the crista parotica; Fig. 1b, c). The tallest (and most ventral) part of the paroccipital process is along the anteromedial aspect, which is best seen in lateral view. The space between the paroccipital process and fenestra vestibuli, within the tympanic cavity, is deeply recessed. A sharp, vertical crest extends medially from the tallest part of the paroccipital process toward the fenestra vestibuli (Fig. 1b, c). The crest is triangular, with a dorsoventrally tall base along the paroccipital process and a pointed tip extending medially toward the fenestra vestibuli. We interpret the crest to be the base of the tympanohyal (Fig. 1). The tympanohyal is part of the hyoid apparatus that, in mammals, fuses with the crista parotica of the petrosal to enclose the hyomandibular branch of the facial nerve (Goodrich 1930). Together with the stylohyoid the tympanohyal forms the styloid process in some mammals (Goodrich 1930). In *Astroconodon* the base of the tympanohyal is continuous with the medial wall of the paroccipital process and there is no apparent gap or hook for the passage of the facial nerve. It is possible that a rod or hook-like extension of the tympanohyal is simply not preserved in MCZ 19973 or MCZ 19974. The tympanohyal is not included in the reconstruction of MCZ 19973 in Crompton and Sun (1985: fig. 7A), but is indicated, although not labeled, in the reconstruction based on MCZ 19973 and MCZ 19969 by Crompton and Luo (1993: fig. 4.12C). The base of the tympanohyal in *Astroconodon* divides the tympanic cavity into a smaller posterior fossa and a larger anterior fossa, both of which are deeply recessed. We agree with Crompton and Luo (1993: fig. 4.12C) and Rougier et al. (1996: fig. 5D) that the posterior fossa represents the stapedius fossa (Fig. 1b, c).

The anterior part of the paroccipital process, lateral to the tympanohyal, forms a thin crest, the crista parotica (Fig. 1b, c). The crista parotica forms the medial border of a deep fossa incudis, which accommodated the crus breve of the incus in life. The fossa incudis is bounded posteriorly by a sharp crest that extends past the fossa incudis ventrally onto the paroccipital process, which is best seen in MCZ 19974. The anterior border is defined by a short ridge between the crista parotica and squamosal in MCZ 19973 and MCZ 19974. The lateral border of the fossa incudis is less well preserved, the squamosal is displaced dorsally, and the whole cranium is dorsoventrally compressed. Despite the poor preservation we suspect that the squamosal formed the lateral border of the fossa incudis. The fossa incudis is the posterior part of a larger space, the epitympanic recess, that accommodates the body of the malleus and incus (MacPhee 1981). The exact outline of the epitympanic recess is difficult to estimate in *Astroconodon* due to the dorsoventral compression in MCZ 19973 and MCZ 19974 and because the area is at least partially obscured by the mandible in MCZ 19974. Nevertheless, the epitympanic recess is best seen in MCZ 19973 and represented by a deep and large depression between the crista parotica of the petrosal medially and squamosal laterally (Fig. 1b).

The crista parotica continues anteriorly past the fossa incudis and tympanohyal roughly to the anteroposterior midpoint of the promontorium, just anterior to the transverse ridge (Fig. 1c). It is separated anteriorly from the lateral flange by a sizeable gap that we here identify as the pterygoparoccipital notch for the ramus superior of the stapedial artery (also referred to as the tympanic opening of the ventral ascending canal or foramen for the ramus superior of the stapedial artery, see for example Rougier et al. (1992) and Wible and Hopson (1995)). This morphology is best seen on the right side of MCZ 19974 (Fig. 1c). Crompton and Sun (1985: fig. 7A) similarly show, but do not label, a long and continuous crista parotica from the paroccipital process to the transverse ridge. The crista parotica is less well preserved and separated by a small gap on the right side of MCZ 19973 (Fig. 1b). This morphology seems to have formed the basis for the reconstruction by Crompton and Luo (1993: fig. 4.12C), which shows the crista parotica ending posterior to the transverse ridge (note the crista parotica is not labeled in their reconstruction). We believe that the gap in MCZ 19973 is a preservational artifact and does not represent the actual morphology. Crompton and Luo (1993: fig. 4.12C) identified what we believe to be an artificial gap within the crista parotica as the pterygoparoccipital notch. In contrast, we place the pterygoparoccipital notch in a more anterior position, between the crista parotica and lateral flange (Fig. 1b, c). There is in fact a gentle curvature to the crista parotica in MCZ 19974 in a similar position to the artificial gap of MCZ 19973. Crompton and Sun (1985: fig. 7A) identified this curvature as the contact for the incus, which we agree with.

Anterior and slightly lateral to the crista parotica is a long and well-developed crest that borders the lateral trough laterally and extends anteriorly to contact the basisphenoid medially (Fig. 1b, c). On the left side of MCZ 19974, this crest bears a lateral bulge adjacent to the anterior part of the lateral trough, with a short zone where a weak midline trough divides the crest into medial and lateral components. We interpret this trough as a probable suture between the lateral flange of the petrosal posteromedially and the quadrate ramus of the alisphenoid anterolaterally. The lateral flange of the petrosal appears to terminate anteriorly at a point adjacent to the foramina at the anterior margin of the lateral trough (anterior opening of cavum epiptericum, carotid foramen and foramen for the inferior ramus of stapedial artery). The lateral, alisphenoid component of the crest continues and broadens anteriorly and medially, forming a weakly-defined, arcuate suture on the lateral side

of the basisphenoid. On the right side of MCZ 19974 the anterior part of the lateral flange is missing, and what we interpret as the quadrate ramus of the alisphenoid remains. No suture is evident on the crest bordering the margin of the lateral trough in MCZ 19973. However, in the zone where we suspect the position of the alisphenoid-petrosal suture, the crest is thickened bilaterally, with an apparent lateral displacement on the right side of MCZ 19973, presumably representing the anterior terminus of the lateral flange of the petrosal. We provisionally identify the lateral crest bordering the lateral trough as a composite structure, with much of the crest being formed by the lateral flange of the petrosal (posteriorly) and a smaller contribution of the quadrate ramus of the alisphenoid (anteriorly). For ease of description, we will refer to the crest as 'lateral flange' here, noting that it includes a small contribution from the alisphenoid. Our interpretation of the crest is most congruent with Crompton and Luo (1993: fig. 4.12C), who labeled the posterior aspect of the crest 'lateral flange', but contrast with Crompton and Sun (1985: fig. 7A) who labeled the same part of the crest 'quadrate ramus of the epipterygoid' (i.e., alisphenoid).

Between the lateral flange and the promontorium is the lateral trough, which forms the floor of the cavum epiptericum. Just anterior to the fenestra vestibuli is an elevated transverse ridge ('tr' in Fig. 1b, c) that passes mediolaterally from the promontorium to the crista parotica. At the midpoint of the transverse ridge are two very small foramina (one anterior and one posterior to the ridge) that connected the venous system surrounding the cochlear canal with the prootic canal (see below). Within the deep lateral trough and posterior to the transverse ridge is the secondary facial foramen (Fig. 1b). The secondary facial foramen is best preserved (although still difficult to see, due to infill) in MCZ 19973. It is barely visible in MCZ 19974 and not preserved in MCZ 19969. We place the foramen in the same position as indicated by Crompton and Luo (1993: fig. 4.12C). The reconstruction by Crompton and Sun (1985: fig. 7A) shows two large foramina, one anterior and one posterior to the transverse ridge, but neither is labeled. The posterior foramen is in a similar position to the secondary facial foramen in Crompton and Luo (1993: fig. 4.12C) and we assume that it represents the opening for the hyomandibular branch of the facial nerve. Tracing of at least part of the passage of the facial nerve was possible in the CT scans of MCZ 19973 and MCZ 19974 and both confirm a placement of the secondary facial foramen posterior to the transverse ridge (Fig. 2a). The facial nerve passed from the internal acoustic meatus, within the petrosal dorsal to the cochlear canal into the cavum supracochleare for the geniculate ganglion dorsal to the lateral trough. In other words, the cavum supracochleare had a bony roof separating it from the endocranium and a bony floor separating it from the lateral trough. In MCZ 19973 the cavum supracochleare is connected to the much larger cavum epiptericum. Alternatively, it is possible that the wall between the cavum supracochleare and the cavum epiptericum was very thin and was damaged in MCZ 19973.

The further course of the facial nerve is less well preserved in the specimens. Typically, the facial nerve divides into two branches: the hyomandibular nerve and the greater petrosal nerve. The hyomandibular nerve passes posteriorly through the secondary facial foramen and leaves the middle ear cavity posterior to the tympanohyal through the stylomastoid notch or foramen. In MCZ 19973 or MCZ 19974, there is no distinct notch or groove within the tympanohyal that the hyomandibular nerve could have hooked around. It is possible that the tympanohyal is incomplete in the two specimens and that a fingerlike projection similar to the one in *Trioracodon* (Wible and Hopson 1993) was in fact also present in *Astroconodon*. The hyomandibular nerve would have passed through a relatively ill-defined stylomastoid notch along the paroccipital process and posterior to the tympanohyal (Fig. 1b, c). In Mesozoic mammaliaforms the greater petrosal nerve is frequently reconstructed to leave the cranium through the hiatus Fallopii in the lateral trough. We were not able to trace any branch from the cavum supracochleare anteriorly toward the lateral trough in MCZ 19973 or MCZ 19974; the only connection anteriorly is to the cavum epiptericum. It is possible that the canal is simply not preserved in any of specimens. Crompton and Sun (1985: fig. 7A) indicate a large foramen anterior to the transverse ridge in the lateral trough that they connect with an arrow with a second foramen posterior to the ridge. Although neither foramen is labeled, we believe that those foramina are intended to represent the secondary facial foramen (posteriorly) and hiatus Fallopii (anteriorly). However, none of the specimens have a large foramen immediately anterior to the transverse ridge and it is also not included in the reconstruction of Crompton and Luo (1993: fig. 4.12C). The position and size as indicated in Crompton and Sun (1985) does not seem feasible given the specimens at hand. We assume that a much smaller opening for the hiatus Fallopii was present within in the lateral trough in life, but that it is not preserved in MCZ 19969, MCZ 19973, or MCZ 19974.

Within the lateral trough, anterior to the hiatus Fallopii, should be a deep recess for the tensor tympani muscle. Rougier et al. (1996: fig. 5D, char. 36/1) identified the tensor tympani fossa in *Astroconodon* in the lateral trough anterior to the crista parotica and medial to the lateral flange (roughly at the position of the 'lt' label in Fig. 1b). We were not able to confirm a distinct fossa in this area, although the labeled position seems reasonable in comparison to the position of the fossa in *Trioracodon* and *Priacodon* (Fig. 4d, e), it does not appear to be a clear and consistent feature in the specimens at hand. On the right side of MCZ 19973, just anterior to the crista parotica, is a slightly rugose, weak eminence that ascends the medial face of the lateral flange, terminating at the floor of the lateral

trough. The medial face of this eminence is weakly concave and may be the fossa for the tensor tympani. The eminence is developed into a low ridge in the lateral trough and running anteromedially, in the same orientation as the crista parotica, on the left side, where no fossa is apparent. Distortion, possible artefacts of mechanical preparation, and bits of mineral infilling render interpretation of MCA 19974 and MZC 19969 problematic.

Deep to the lateral trough is the cavum epiptericum. Much of the cavum epiptericum had a bony floor except for the very anterior portion, which contains a small anterior opening into the cavum epiptericum (Fig. 1b, c). Laterally, the cavum epiptericum opens along the lateral wall of the braincase with a large foramen for cranial nerves V2 and V3. Posteriorly, it appears that the cavum epiptericum was confluent with cavum supracochleare. In MCZ 19973 there are three foramina at the anterior end of the lateral trough (Fig. 1b). The foramina at the anterior end of the lateral trough are less well preserved in MCZ 19974 and MCZ 19969 (Fig. 1c, d). Crompton and Sun (1985: fig. 7A) and Crompton and Luo (1993: fig. 4.12C) also figured three foramina in the anterior end of the lateral trough. None of these foramina at the anterior end of the lateral trough was labeled by either Crompton and Sun (1985: fig. 7A) or Crompton and Luo (1993: fig. 4.12C). The most medial foramen is present bilaterally in MCZ 19973 (Fig. 1b). The foramen is circular in outline and a short groove leads to the foramen posteriorly. The foramen is also present in MCZ 19974, in which it is more visible on the left side but barely recognizable on the right side. The foramen appears larger in MCZ 19973 than in MCZ 19974, perhaps because of more complete preparation or preservation. This foramen is positioned between the petrosal and basisphenoid, and appears to lead medially into the cranium. We believe that this medial-most foramen at the anterior end of the lateral trough represents the opening for the internal carotid artery (i.e., carotid foramen). The other two foramina sit in a depression that is separated from the carotid foramen by a bony septum (Fig. 1b). The two lateral foramina are best seen on the right side of MCZ 19973, but are also visible on the left side of the same specimen (Fig. 1b). In MCZ 19974 two lateral foramina are preserved on the left side, but only one lateral foramen is visible on the right side (Fig. 1c). The more posterior foramen is much larger than the carotid foramen, has an oval outline, and appears to lead into the endocranial cavity. We could not clearly trace a connection to the cavum epiptericum in the µCT scans, but this foramen likely represent the anterior opening into the cavum epiptericum (Fig. 1b, c). The anterolateral foramen appears rounder and opens into a canal that passes anteriorly and laterally. On the right side of MCZ 19974 the foramen and canal open laterally with the foramen for V2 and V3 on the lateral braincase wall. We interpret this anterolateral foramen to be the conduit for the ramus inferior of the stapedial artery. In MCZ 19973 there is another opening in the lateral trough on the right side that is most likely an artifact of damage or preparation rather than an actual foramen (asterisk in Fig. 1b).

The tympanic opening of the prootic canal is lateral to the crista parotica and separated from the pterygoparoccipital notch (Fig. 1b). Crompton and Luo (1993: fig. 4.12C) and Crompton and Sun (1985: fig. 7A) both identified the tympanic opening of the prootic canal in the same position. Reconstructing the course of the prootic canal is, however, difficult. The canal can only be traced for a short distance into the petrosal but not to its endocranial opening. The endocranial opening of the prootic canal is scored as in the 'rear of the cavum epiptericum' for *Trioracodon* and 'between the cavum [epiptericum] and anterodorsal margin of [the] subarcuate fossa' in *Priacodon* and *Triconodon* by Rougier et al. (1996: char. 26). From what can be reconstructed in *Astroconodon*, it is unclear whether the prootic canal would have opened into the cavum epiptericum or into the endocranial cavity directly. It appears that some of the smaller canals of the hypocochlear sinus (see below), that open into the lateral trough close to the transverse ridge connect to the prootic canal internally (Fig. 2). There are no distinct grooves for the lateral head vein, but we suspect that the post-trigeminal vein and prootic sinus formed the lateral head vein within the lateral trough.

Vasculature

An extensive network of well-preserved vascular canals surrounds the cochlear canal within the petrosal in *Astroconodon* (Figs. 2 and 3). The largest of these vascular canals (or network of canals) extends along the medial margin of the cochlear canal and would have contained the inferior petrosal sinus (Fig. 2). The inferior petrosal sinus left the petrosal through a foramen anterior to the perilymphatic foramen (Fig. 1c). The number and size of the canals for the inferior petrosal sinus are variable in *Astroconodon*. In MCZ 19973, a single large canal is preserved bilaterally (Fig. 2b). In contrast, there are at least three canals on the right side and two on the left of MCZ 19974 that appear to represent the inferior petrosal sinus (Fig. 2e). Several smaller canals cross the ventral surface of the cochlear canal anterior to the perilymphatic foramen. Harper and Rougier (2019) described those canals as the 'hypocochlear sinus', which we follow here. While there are numerous smaller canals for the hypocochlear sinus that anastomose in MCZ 19974 (Fig. 2e), there appear to be fewer but larger canals for the hypocochlear sinus in MCZ 19973 (Fig. 2b). Although preservation might influence the exact number of the hypocochlear and inferior petrosal sinus canals in *Astroconodon*, at least some of the differences appear to be attributable to

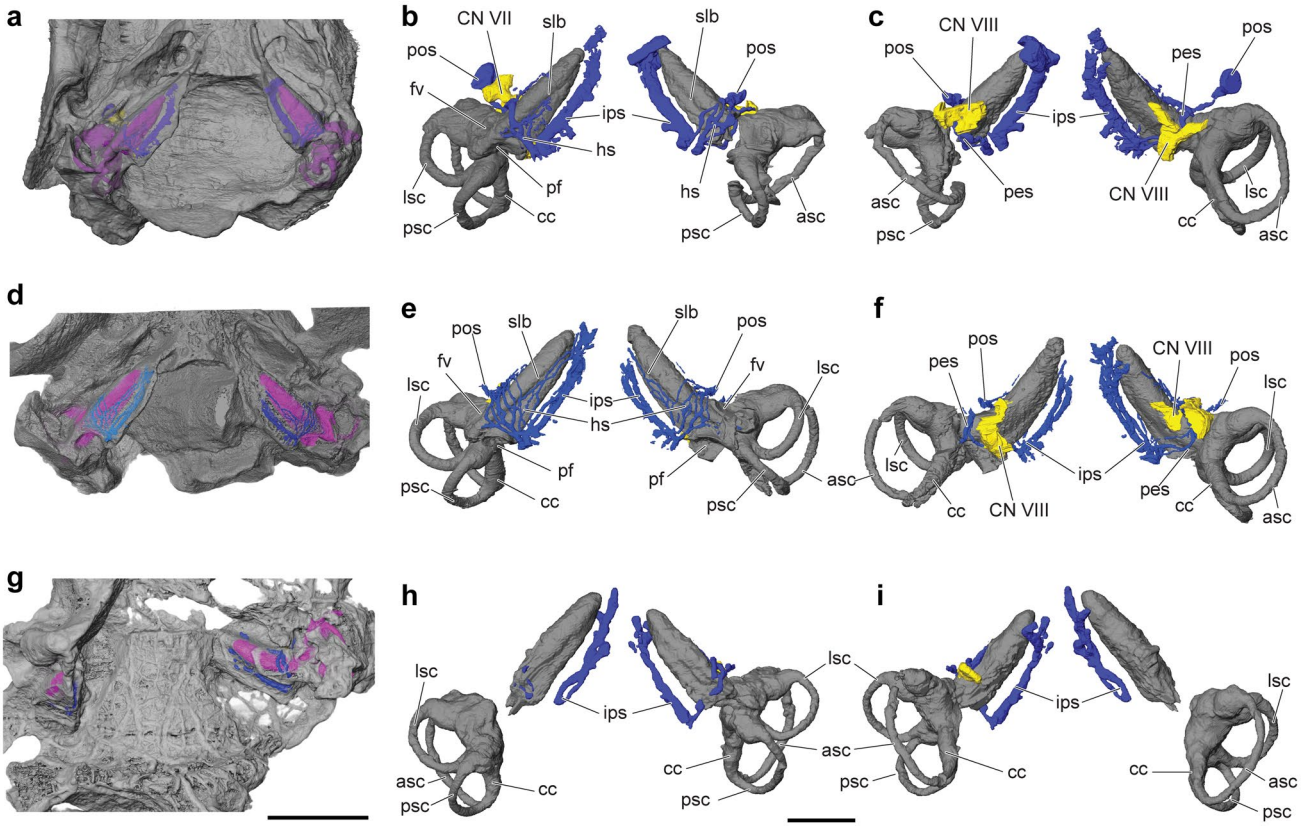

Fig. 2 Rendering of 3D virtual model of inner ears of *Astroconodon* sp. based on µCT data of **a–c**. MCZ 19973; **d–f**. MCZ 19974; **g–i**. MCZ 19969. **a**, **b**, **c**, position of inner ear (pink) and vasculature (blue) in ventral view of semi-transparent basicranium. **b**, **e**, **h** ventral view of inner ear (gray), vasculature (blue), and nerves (yellow), right inner ear on the left, left inner ear on the right. Facial nerve (CN VII) shown in ventral view of right inner ear of MCZ 19973 (**b**) but removed in dorsal view (**c**) to show passage of the epicochlear sinus. **c**, **f**, **i**, dorsal view of inner ear (gray), vasculature (blue), and nerves (yellow), right inner ear on the right, left inner ear on the left. Abbreviations: **asc**, anterior semicircular canal; **cc**, crus commune; **CN VII**, facial nerve; **CN VIII**, vestibulocochlear nerve; **fv**, fenestra vestibuli; **hs**, hypocochlear sinus; **ips**, inferior petrosal sinus; **lsc**, lateral semicircular canal; **pcs**, posterior semicircular canal; **pes**, posterior epicochlear sinus; **pf**, perilymphatic foramen; **pos**, prootic sinus; **slb**, secondary osseous lamina base. Scale equals 5 mm in **a**, **d**, **g** and 2 mm in **b**, **c**, **e**, **f**, **h**, and **i**

intraspecific variation in morphology. In MCZ 19974 two smaller vascular canals pass from the hypocochlear sinus anteriorly within the groove for the base of the secondary osseous lamina (sensu Schultz et al. 2017; see below). However, none of the canals of the hypocochlear sinus appear to open into the cochlea directly. The canals for the hypocochlear sinus connect laterally to the prootic canal (Fig. 2b, e). On the dorsal surface of the cochlea (Fig. 2c, f) the canals for the inferior petrosal sinus and prootic sinus also connect through one or two posterior epicochlear sinus canals sensu Harper and Rougier (2019) ('transcochlear sinus' in Panciroli et al. 2019). The posterior epicochlear sinus canals pass posterior to the entry of the cochlear nerve. A canal for the anterior epicochlear sinus appears to be absent or is too small or not well enough preserved to be recognized in the CT scans of *Astroconodon* (Figs. 2c, f and 3). The canals for the hypocochlear and epicochlear sinuses connect along the lateral aspect of the cochlear canal, where they either open into the lateral trough through the small foramina along the transverse ridge or connect to the prootic canal.

We reconstruct the prootic sinus to have passed extracranially from the tympanic opening of the prootic canal into the lateral trough, where it would have likely met with the post-trigeminal vein to form the lateral head vein. We reconstruct the post-trigeminal vein to have entered the lateral trough through the anterior opening of the cavum epiptericum. The post-trigeminal vein would have traveled posteriorly within the lateral trough to meet the prootic sinus.

There are no clear grooves in the lateral trough or on the promontorium to indicate the course of the internal carotid artery or the stapedial artery and its branches. We suspect that the internal carotid artery passed

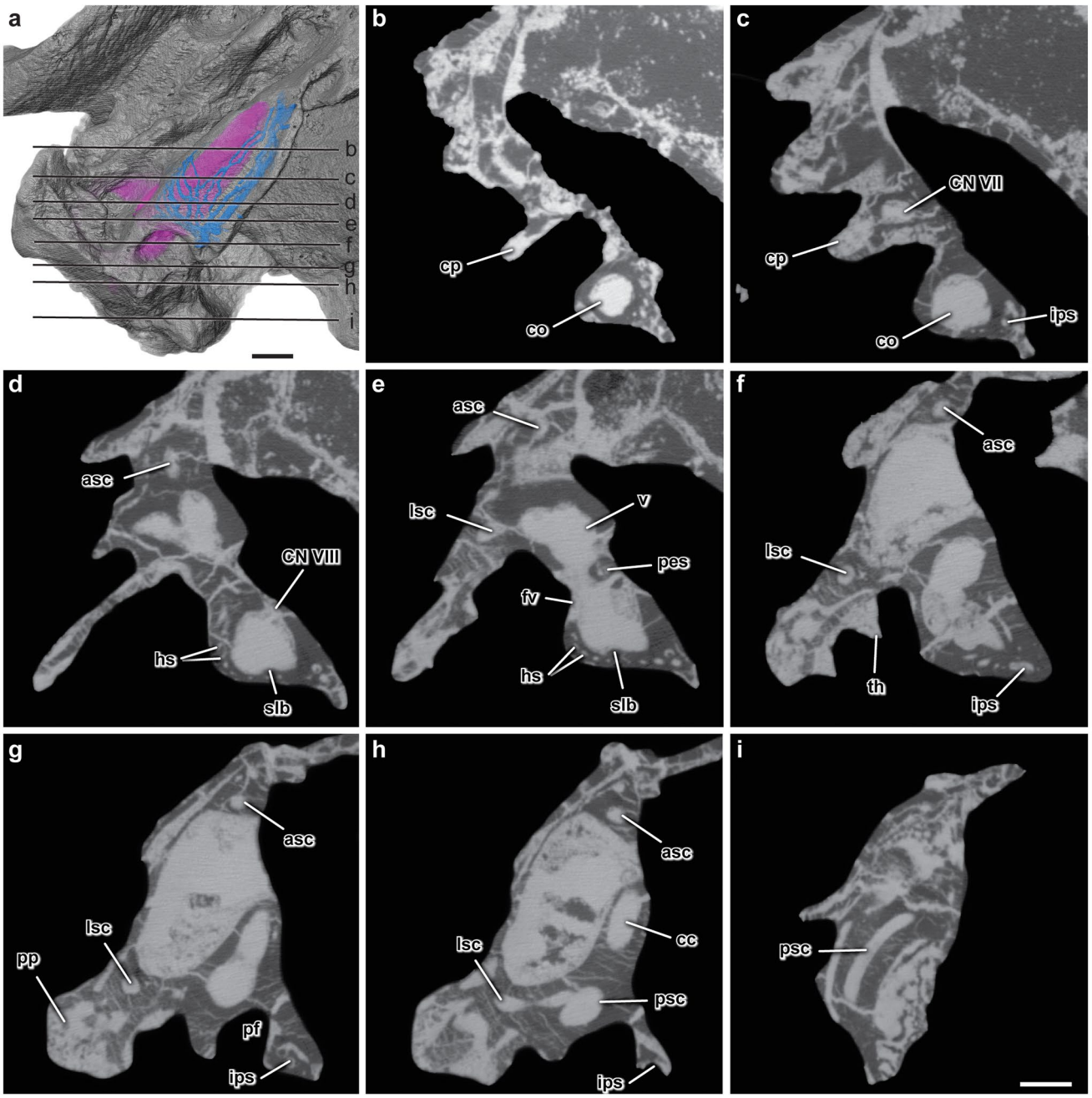

Fig. 3 Serial slices through right petrosal of *Astroconodon* sp. (MCZ 19974) obtained via µCT imaging. Position of each transverse slice (**b**–**i**) is indicated in ventral semi-transparent view of cranium in **a.** Abbreviations: **asc**, anterior semicircular canal; **cc**, crus commune; **CN VII**, facial nerve; **CN VIII**, vestibulocochlear nerve; **co**, cochlear canal; **cp**, crista parotica; **fv**, fenestra vestibuli; **hs**, hypocochlear sinus; **ips**, inferior petrosal sinus; **lsc**, lateral semicircular canal; **pcs**, posterior semicircular canal; **pes**, posterior epicochlear sinus; **pf**, perilymphatic foramen; **pp**, paroccipital process; **slb**, secondary osseous lamina base; **th**, tympanohyal; **v**, vestibule. Scale bar equals 1 mm in **a** and 0.5 mm in **b**-**i**

through the carotid foramen at the anterior aspect of the lateral trough into the cranial cavity. The stapedial artery would have likely split into an inferior and superior ramus within the middle ear cavity, with the inferior ramus traveling anteriorly with the post-trigeminal vein and the superior ramus passing laterally through the pterygoparoccipital notch. The superior ramus would have then passed into the ventral ascending channel where it would have anastomosed with the much larger arteria diploëtica magna. The most ventral portion of the

ventral ascending channel appears to be a laterally open groove in *Astroconodon*.

Inner ear

The endocasts of the inner ear are well preserved in MCZ 19973 and MCZ 19974 (Fig. 2). The most intact inner ear is that on the right side of MCZ 19974, which will serve as the primary source for the description provided here (Figs. 2d–f and 3). The right inner ear of MCZ 19973 is likewise well preserved but the smaller vascular canals surrounding the cochlear canal are less visible (Fig. 2b, c). The vestibule and semicircular canals of the left side in MCZ 19973 and MCZ 19974 sustained some damage, more so in MCZ 19973 than in MCZ 19974. The inner ear is least well preserved in MCZ 19969 (Fig. 2g–i), with substantial damage to the cochlear canal and vestibule on the right side. In all three specimens the osseous labyrinth and associated vessels are completely infilled with dense matrix.

The cochlear canal is slender and straight in ventral view (Fig. 2b, e, h). In posteromedial view the cochlear canal is very gently bent, with the greater curvature facing ventrolaterally or abneural and the lesser curvature facing dorsomedially or neural. The curvature of the cochlear canal is so slight that it is difficult to measure with any accuracy. The cochlear canal is between 3.6 and 4.1 mm in length, or about 8.4% of cranial length in MCZ 19973 (Table 1). It extends the complete length of the promontorium (Fig. 2a, d, g). The cochlear canal tapers anteriorly, with a very slight constriction at the most anterior tip of the canal. There is no apical expansion or distinct canal for the lagenar nerve. A distinct groove for the base of the secondary lamina is present on the ventral surface of the cochlear canal endocast. The secondary lamina base is visible in cross sections as a low ridge on the inner surface of the cochlear canal (Fig. 3d, e). The secondary lamina base extends nearly the complete length of the cochlear canal, running from the posterior aspect of the perilymphatic foramen to the apical constriction of the cochlear canal. A primary osseous lamina, osseous cochlear ganglion canal and cribriform plate are lacking in all specimens so that the surface of the canal is smooth. There is a single cochlear nerve foramen on the neural aspect of the cochlear canal. The radii of curvature of the semicircular canals differ. The anterior semicircular canal has the largest arc and the lateral semicircular the smallest (Table 1). The anterior and posterior semicircular canal meet to form a primary crus commune. The lateral and posterior canal remain distinct and do not merge close to the posterior ampulla. A secondary crus commune is therefore absent.

Comparison and discussion

Petrosal

The comparison focuses on the well described and illustrated petrosals of *Priacodon* (Rougier et al. 1996; Harper and Rougier 2019; Fig. 4d), *Trioracodon* (Kermack 1963; Fig. 4e) and *Triconodon* (NHM 47763, Simpson 1928; Kermack 1963; Fig. 4f) and scorings of those petrosals in Rougier et al. (1996). Several other eutriconodontans or taxa closely affiliated with eutriconodontans (i.e., 'amphilestids') preserve the basicranial region but their descriptions are cursory and/or lack detailed images. Among those, the 'amphilestid' *Juchilestes* is most thoroughly described (Gao et al. 2010: Supplementary Material) but the illustrations of the cranium (Gao et al. 2010: fig. 1) are not detailed enough to confirm or evaluate the basicranial morphology. Despite its contentious placement as an 'amphilestid' outside of Eutriconodonta (Rougier et al. 2021: fig. 5.1) we are including comparisons to *Juchilestes* and other 'amphilestids' here when feasible. In addition, the petrosal region is preserved in *Spinolestes* (Martin et al. 2015: fig. ED 1) and *Liaoconodon* (Meng et al. 2011: figs. S1, S2) but comparison is mainly based on the character scorings of *Spinolestes* in Martin et al. (2015) and *Liaoconodon* in Mao et al. (2020) because descriptions and illustration lack sufficient detail. Likewise, the several well-preserved crania for *Gobiconodon* (Li et al. 2003) and *Repenomamus* (*R. robustus*, Li et al. 2001: fig. 1B, Wang et al. 2001: fig. 1A–C; *R. giganticus*, ventral view not figured: Hu 2006, and five crania of *Repenomamus*, not figured: Hu 2006) are only partially described. Our comparison to *Gobiconodon* and *Repenomamus*, thus relies heavily on scorings in Hu (2006) and Martin et al. (2015). In addition, the promontorium is indicated in *Jueconodon* (Mao et al. 2021: fig. ED6) but the basicranium is damaged in the holotype and only known specimen and most characters regarding the petrosal or inner ear are scored as 'unknown' by Mao et al. (2021).

The shape of the promontorium is essentially the same in *Priacodon*, *Trioracodon*, *Triconodon*, and *Astroconodon*. It is long and slender and scored or described as 'finger-like' by Rougier et al. (1996: char. 3). Although the ventral surface of the promontorium is damaged in *Juchilestes*, Gao et al. (2010: p. 241) expressed "no doubt that it has a cylindrical and finger-like form". The ventral surface of the promontorium is also scored as 'elongate and cylindrical' for *Gobiconodon*, *Repenomamus*, *Jeholodens*, *Liaoconodon*, and *Spinolestes* (Gao et al. 2010: char. 304; Martin et al. 2015: char. 352; Mao et al. 2020: char. 362). Though slightly

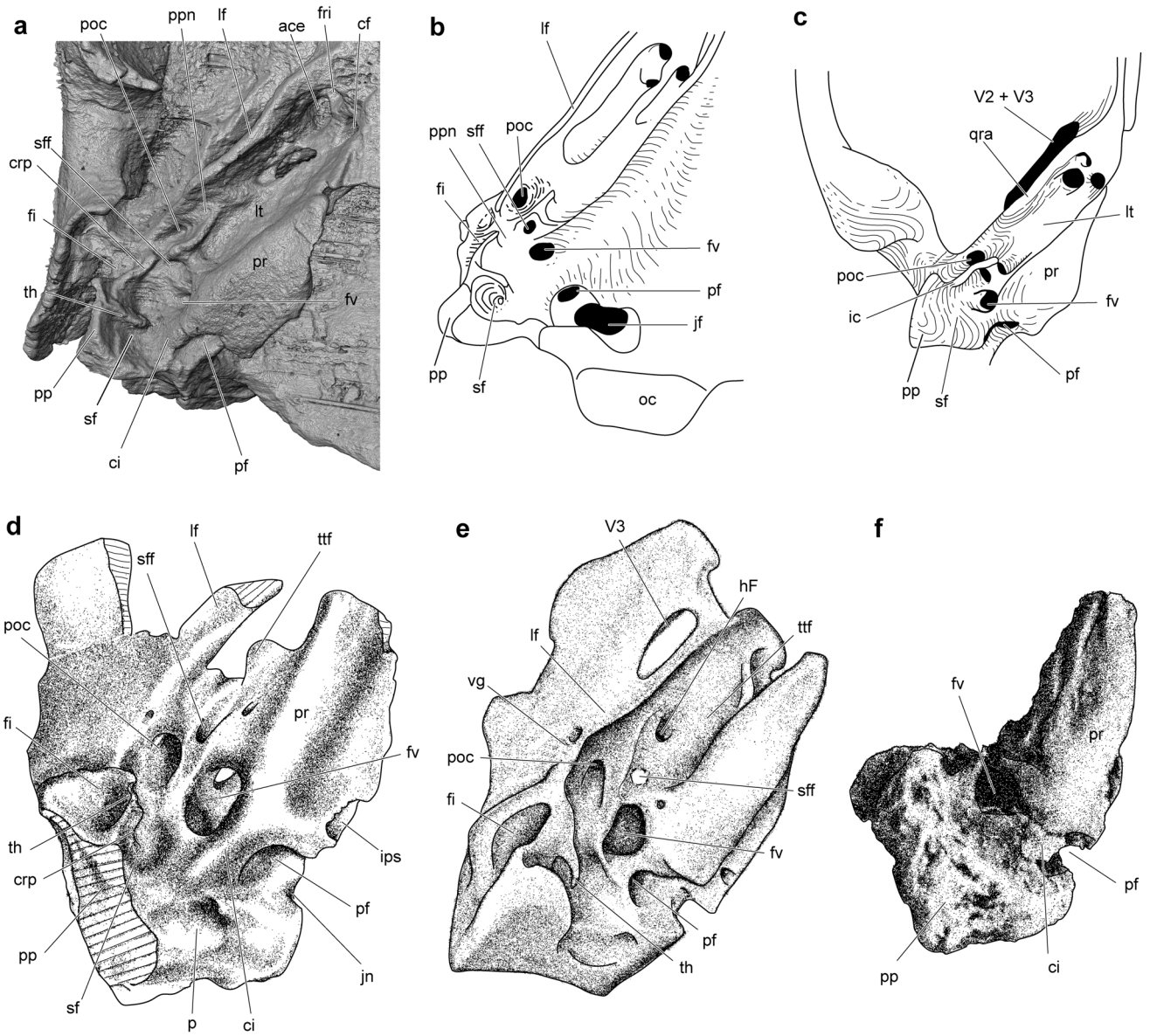

Fig. 4 Comparison of triconodontid petrosal morphology. **a**. *Astroconodon* sp. (MCZ 19973, this study); **b**. *Astroconodon* sp. (modified from Crompton and Luo 1993); **c**. *Astroconodon* sp. (modified from Crompton and Sun 1985); **d**. *Priacodon* (modified from Rougier et al. 1996); **e**. *Trioracodon* (modified from Wible and Hopson 1993); and **f**. *Triconodon* (modified from Kermack 1963). Labels in **b**–**f** represent original identification of morphology by various authors and not our interpretation. Abbreviations: **ace**, anterior opening of cavum epiptericum; **cf**, carotid foramen; **ci**, crista interfenestralis; **crp**, crista parotica; **fi**, fossa incudis; **fri**, foramen for inferior ramus of stapedial artery and post-trigeminal vein; **fv**, fenestra vestibuli; **hF**, hiatus Falloppii; **ips**, inferior petrosal sinus; **ic**, incus contact; **jf**, jugular foramen; **jn**, jugular notch; **lf**, lateral flange; **lt**, lateral trough; **oc**, occipital condyle; **p**, 'pocket'; **pe**, petrosal; **pf**, perilymphatic foramen; **pp**, paroccipital process; **ppn**, pterygoparoccipital notch; **pr**, promontorium; **poc**, tympanic opening of prootic canal; **qra**, quadrate ramus of alisphenoid [i.e. epipterygoid]; **sf**, stapedial fossa; **sff**, secondary facial foramen; **th**, tympanohyal; **tr**, transverse ridge; **ttf**, tensor tympani fossa; **V2**, opening for maxillary division of trigeminal nerve; **V3**, opening for mandibular division of trigeminal nerve; **vg**, vascular groove. Images not to same scale

displaced, the right promontorium in *Jueconodon* appears to have an elongate shape (Mao et al. 2021: fig. ED6). Nevertheless, Mao et al. (2021: char. 404) scored the external outline of the promontorium as 'unknown' for *Jueconodon*. The right promontorium seems more rounded in *Spinolestes* than the slender promontoria of the triconodontids *Priacodon*, *Trioracodon*, *Triconodon*, and *Astroconodon*, at least based on Extended Data Figure 1 in Martin et al. (2015). Without having seen the original specimen, it is difficult to assess whether the promontorium differs from those of other eutriconodontans. Martin et al. (2015: p. Supplementary Material 11) described the promontorium as "cylindrical". In other

gobiconodontids the promontorium is described as "elongated cone-shaped" (*Gobiconodon* – Li et al. 2003: p. 1131), "elongated" (*Repenomamus* – Wang et al. 2001: p. 359) or "finger-shaped" (*Repenomamus* – Li et al. 2001: p. 783). Aside from the slight variation in wording between different authors and character matrices, we believe that the shape of the promontorium is generally conserved in gobiconodontids and triconodontids and that eutriconodontans share an elongate and slender promontorium.

Astroconodon retains the plesiomorphic condition for mammaliaforms of a perilymphatic foramen with a distinct and open perilymphatic groove. In extant therians the perilymphatic foramen and perilymphatic duct are separated during development by the bony processus recessus, which leads to the formation of the fenestra cochleae and aqueductus cochleae for the perilymphatic duct (Zeller 1993). Several linages of eutriconodontans independently closed or partially covered the perilymphatic groove by bony lappets, creating an incomplete or complete processus recessus. The best documented example of bony lappets forming a processus recessus in eutriconodontans is perhaps that of *Priacodon*. Rougier et al. (1996: p. 5, 15, fig. 2) described the perilymphatic groove in *Priacodon* as "nearly closed" by "bony lappets on the edges of the sulcus" and included detailed drawings. This description is supported by Harper and Rougier (2019: p. 22) more recently, who noted that an "incipient expression of an incomplete 'processus recessus' has also been recognized in *Priacodon.*" In addition, the perilymphatic groove is scored as 'at least partially enclosed' in *Trioracodon*, *Priacodon*, *Gobiconodon*, *Repenomamus* and *Spinolestes* in various data sets (Hu 2006: char. 237; Martin et al. 2015: char. 401; Mao et al. 2020: char. 408). By comparison, the scorings in Rougier et al. (1996) distinguish between four character states for the perilymphatic groove: 'no indication', 'open sulcus', 'partially enclosed by bony lappets', and 'fully enclosed to form a canal, a cochlear aqueduct'. Rougier et al. (1996: char. 11) scored *Priacodon* as 'partially enclosed', *Trioracodon* as 'open sulcus' and 'partially enclosed' and *Triconodon* and the 'Cloverly triconodonts' as 'unknown'. Although *Trioracodon* is scored in more recent matrices as having an at least 'partially closed perilymphatic groove', Rougier et al. (1996: p. 15) were less certain, noting that a "sulcus is also present in *Trioracodon* (Kermack 1963: fig. 3), but the presence of bony lappets is uncertain from the published figures." In the original description of the *Trioracodon* petrosal, Kermack (1963: p. 86) is more assertive, stating that "There is no sign of an aquaeductus cochleae, and it is quite certain that one did not exist, as the relevant part of the petrosal is quite undamaged and free from cracks." This statement is supported by Wible and Hopson (1993: char. 34), who scored the perilymphatic groove as 'open' in Triconodontidae. Wible and Hopson (1993) did not explicitly list which taxa they included in the composite Triconodontidae, but *Trioracodon* is figured and referenced frequently as an example and Kermack (1963), Crompton and Sun (1985) and Crompton and Luo (1993) are cited as sources for the scorings. These factors suggest that Wible and Hopson's (1993) scoring is based on *Trioracodon* (Kermack 1963), *Triconodon* (Kermack 1963) and *Astroconodon* (Crompton and Sun 1985; Crompton and Luo 1993). Rougier et al. (1996: p. 15) scored *Triconodon* and *Astroconodon* (the unnamed 'Cloverly triconodonts') as 'unknown' and stated that the "appropriate part of the petrosal is not preserved, described or figured." We agree that the morphology in *Triconodon* is not preserved or not recognizable in published figures (Kermack 1963: figs. 8, 9; Simpson 1928: fig. 25) and should be treated as unknown. However, based on the high-resolution CT scans of *Astroconodon*, we can confirm that the groove was not covered by bony lappets. The perilymphatic groove is present in MCZ 19973 and MCZ 19969. This groove is deeper in MCZ 19969 than in MCZ 19973, but there is no evidence that the perilymphatic duct was fully or partially enclosed in bone in any of the specimens.

Harper and Rougier (2019: p. 40) indicated that the enclosure of the perilymphatic duct is much more extensive in Gobiconodontidae, paralleling the morphology in therians with "a well-developed processus recessus, fenestra cochleae, and aqueductus cochleae". Despite this fact the foramen is still labeled or described as perilymphatic foramen and not as fenestra cochleae in Wang et al. (2001: fig. 2) and Li et al. (2003). The evidence for a fenestra cochleae is inconclusive for *Juchilestes*. Gao et al. (2010) described the foramen as 'foramen cochleare' which would imply that the perilymphatic grove is closed and a process recessus present, but these authors also scored *Juchilestes* as having an open perilymphatic groove (Gao et al. 2010: char. 350). The condition of the perilymphatic groove is scored as 'unknown' for *Liaoconodon*, *Jeholodens*, *Yanoconodon* (Mao et al. 2020: char. 408), and *Jueconodon* (Mao et al. 2021: char. 451). In sum, growth of appositional bone from the rear of the otic capsule seems to have occurred independently in several eutriconodontans separating, to a variable degree, the perilymphatic duct from the remainder of the middle ear cavity. The most complete enclosure of the perilymphatic duct is known in Gobiconodontidae with a well-developed aqueductus cochleae similar to that of therians. The morphology varies even within the closely related Triconodontidae, with *Priacodon* exhibiting a partial closure of the perilymphatic groove, whereas the perilymphatic groove remains open in *Trioracodon* and *Astroconodon*.

We can confirm the placement of the stapedius fossa posterior to the tympanohyal and lateral to the crista interfenestralis in *Astroconodon*, as first indicated by Crompton

and Luo (1993: fig. 4.12C). Rougier et al. (1996: figs. 1D and 5D) likewise placed the stapedius fossa posterior to the tympanohyal and lateral to the crista interfenestralis in *Priacodon* and *Astroconodon*. Wible and Hopson (1993) originally identified the stapedius fossa in *Trioracodon* as medial to the paroccipital process and posteromedial to the crista interfenestralis (labeled 'pocket' in *Priacodon* by Rougier et al. 1996). Rougier et al. (1996) revised this identification in *Trioracodon*, stating that the stapedius fossa is present lateral to the crista interfenestralis as in *Priacodon*. The equivalent area to the 'pocket' of *Priacodon* and *Trioracodon* is not preserved in MCZ 19969, MCZ 19973, or MCZ 19974 and it is unclear if this feature is more broadly present in Triconodontidae.

The paroccipital process is well preserved and complete on the right side of MCZ 19973 and nearly complete in MCZ 19974. A complete paroccipital process is also known for *Trioracodon* (Wible and Hopson 1993: Fig. 5.3B). In both triconodontids the paroccipital process extends ventrally past the surface of the promontorium. A ventrally projecting paroccipital process is also scored as 'present' in *Priacodon* and *Triconodon* by Rougier et al. (1996: char. 17), and in *Gobiconodon*, *Repenomamus*, *Liaoconodon* and *Spinolestes* by Hu (2006: char. 255), Mao et al. (2020: char. 393) and Martin et al (2015: char. 383). Even though the paroccipital process is broken at its base in *Priacodon* and *Triconodon*, it is very likely that the process would have extended ventrally past the surface of the promontorium given that the preserved base is at the level of the promontorium.

A tympanohyal is known in several eutriconodontans, including *Astroconodon*, *Trioracodon* (Wible and Hopson 1993), *Priacodon* (Rougier et al. 1996), *Repenomamus* (Wang et al. 2001: fig. 2), and *Liaoconodon* (Meng et al. 2011: Supplementary Material). In these taxa, the tympanohyal is located medial to the paroccipital process, points toward the fenestra vestibuli, and does not reach or contact the promontorium. Only the base of the tympanohyal is preserved in *Priacodon* and *Liaoconodon* and based on the reconstruction in Wang et al. (2001), the shape and completeness of the tympanohyal in *Repenomamus* is difficult to assess beyond the observation that it is slender and points posteromedially. Of the eutriconodontans, the tympanohyal appears most complete in *Trioracodon*, where it is slender with a distinct hook-like appearance. In comparison, the tympanohyal is more robust in *Astroconodon* than in *Trioracodon*; the base is taller dorsoventrally and forms a solid ridge rather than a hook-like process. It is likely that a hook-like or rod-like extension of the tympanohyal was present in *Astroconodon*, but is simply not preserved in the specimens at hand.

Extending anteriorly from the paroccipital process is the crista parotica in Triconodontidae and other eutriconodontans. The crista parotica is part of the ancestral craneo-quadrate joint and is universally present in early mammaliaforms and as such in eutriconodontans. In *Astroconodon* the crista parotica is relatively long, extending past the level of the fenestra vestibuli and roughly to the anteroposterior midpoint of the promontorium. The crista parotica is much shorter in *Priacodon* in which the sharp crest ends at the anterior level of the fenestra vestibuli. Although not labeled in Wible and Hopson (1993: fig. 5.3B) a crista parotica is preserved in *Trioracodon* (Rougier et al. 1996). Kermack (1963: p. 89, figs. 4, 5, 6, 14) already noted the presence of a crest between the fossa incudis and the pterygoparoccipital notch in *Trioracodon* that he termed the 'posterior part of lateral flange'. The crest is in the same position as the crista parotica of other triconodontids and should be more appropriately referred to as a crista parotica. Similar to *Priacodon*, the crista parotica ends at the anterior level of the fenestra vestibuli. A crista parotica is also scored as 'present' or crest-like in *Gobiconodon*, *Repenomamus*, and *Liaoconodon* by Hu (2006: char. 249) and Mao et al. (2020: char. 394), but its length is not scored or discussed.

In *Astroconodon* and other eutriconodontans the crista parotica is separated from the lateral flange anteriorly by a large pterygoparoccipital notch (variously also referred to as the tympanic opening of the ventral ascending channel or foramen for the superior ramus of the stapedial artery, Fig. 4a). Our interpretation of the position of the pterygoparoccipital notch in *Astroconodon* differs from that in Crompton and Luo (1993), who placed the notch more posteriorly within the crista parotica at the level of the fenestra vestibuli and medial to the position of the fossa incudis (Fig. 4b). The same curvature of the crista parotica is indicated by Crompton and Sun (1985) as the contact for the incus (Fig. 4c), which we believe to be a more reasonable interpretation of the morphology. A pterygoparoccipital notch between the crista parotica and lateral flange has been described or imaged in a range of eutriconodontans. Rougier et al. (1996: p. 22) first identified a "wide separation between the crista parotica and the lateral flange" as an unequivocal synapomorphy of Triconodontidae and scored it as such in *Priacodon*, *Trioracodon*, and *Astroconodon* i.e., the 'Cloverly triconodonts' (char. 30). In more recent matrices, scorings for eutriconodontans have changed to 'narrowly separated' by Mao et al. (2020: char. 389 in *Gobiconodon*, *Repenomamus*, and *Priacodon,* scored 'unknown' for *Trioracodon*) and Martin et al. (2015: char. 379 in *Gobiconodon*, *Repenomamus*, *Spinolestes*, and *Priacodon,* scored 'unknown' for *Trioracodon*). Tracing back iterations of the matrices used by Mao et al. (2020) and Martin et al. (2015), it appears that Luo et al. (2002: char. 210) first indicated a 'narrow separation' for the eutriconodontans, scoring *Priacodon* and *Trioracodon* the same as *Morganucodon*, *Megazostrodon*, and *Dinnetherium*, in contrast to the 'wide separation'

seen in non-mammaliaform cynodonts. Because the terms 'narrow' and 'wide' are not further qualified in any of the matrices, evaluating the size of the separation and comparing it between different species is dependent on the observer. The separation between the lateral flange and crista parotica is similar in morganucodontans and at least *Repenomamus*. In *Astroconodon* the gap between the crista parotica and lateral flange appears wider due to the fact that the lateral flange and crista parotica gently decrease in height and do not form a distinct semicircular notch as they do in *Repenomamus*.

The reason for the change in scorings for *Trioracodon* from 'separated' in Rougier et al. (1996) and Luo et al. (2002) to 'unknown' in recent matrices (e.g., Martin et al. 2015; Mao et al. 2020) is less clear. It appears that Luo et al. (2003: char. 296) first scored this character as 'unknown' for *Trioracodon*, which was then followed in the various iterations of this matrix leading up to Mao et al. (2020). Original photographs of the specimens in Kermack (1963: fig. 3) show a gap between the crista parotica (his 'posterior part of the lateral flange') and the lateral flange (his 'anterior part of the lateral flange'). In addition, Kermack (p. 87) also described the lateral flange in *Morganucodon* as "interrupted, as in *Trioracodon*, at about the level of the fenestra ovalis." Wible and Hopson's reconstruction (1993: fig. 5.3B) appears to show a continuous crest from the paroccipital process to the lateral flange, but the ventral view might simply not be conducive to illustrating the gap between the crista parotica and lateral flange in *Trioracodon*. Rougier et al. (1996: fig. 5E, char. 30/1), in addition to the scorings, also indicate a wide separation between the crista parotica and lateral flange at the level of the fenestra vestibuli just anterior to the tympanohyal in *Trioracodon*. We therefore follow Kermack (1963), Rougier et al. (1996) and Luo et al. (2002) and treat the crista parotica and lateral flange as separated in *Trioracodon*. Even though the pterygoparoccipital notch is present between the crista parotica and lateral flange in *Priacodon*, *Trioracodon* and *Astroconodon*, the relative position of the notch differs. In *Priacodon* and *Trioracodon* the pterygoparoccipital notch is at the level or just anterior to the fenestra vestibuli, whereas it is farther anterior in *Astroconodon,* roughly at the anteroposterior midpoint of the promontorium (Fig. 4).

Further, Gao et al. (2010) scored the crista parotica as 'continuous' with the lateral flange in *Juchilestes*. Assessing this morphology is not possible based on Figure 1 in Gao et al. (2010). The lateral trough and lateral flange are present in *Juchilestes* and possibly the edge of the pterygoparoccipital foramen, but it is unclear how much of the crista parotica is preserved because the paroccipital process is broken away. In fact, Gao et al. (2010) scored most characters pertaining to the crista parotica as 'unknown'. We are not convinced that the size and morphology of the crista parotica can be accurately assessed in this specimen and we treat *Juchilestes* as 'unknown' for this feature.

In *Astroconodon*, as in most other eutriconodontans, the pterygoparoccipital foramen takes on the form of an open notch in the petrosal. A laterally open pterygoparoccipital notch is a basal feature in mammaliamorphs and is present in tritylodontids, *Brasilodon*, *Sinoconodon*, and morganucodontans. The pterygoparoccipital foramen/notch is scored as 'laterally open' in *Repenomamus*, *Gobiconodon* and *Priacodon* by Mao et al. (2020: char. 391). Luo et al. (2002: char. 211) and Rougier et al. (2007: char. 211) also scored the foramen as 'open notch' in *Trioracodon* while it is scored as 'unknown' by Mao et al. (2020). Mao et al. (2020)'s scoring as well as previous iterations of this matrix might have been influenced by the reconstruction of the petrosal of *Trioracodon* in Wible and Hopson (1993: fig. 5.3B), which did not indicate the presence of a pterygoparoccipital notch or foramen. Kermack (1963: fig. 3) did not label the pterygoparoccipital notch either, but notes that what he described as the posterior part of the lateral flange (i.e. the crista parotica) forms the "border of the deep pit (lateral pit) [i.e. fossa incudis] which forms one of the walls of the foramen pterygoparoccipitale" (p. 87). Although the terminology differs, Kermack's description mirrors the morphology in *Priacodon*, which has a gap for the pterygoparoccipital notch between the lateral flange anteriorly and the crista parotica posteriorly. Kermack's (1963) description and early scorings by Luo et al. (2002) and Rougier et al. (2007) are convincing that an open notch is indeed present in *Trioracodon,* and that the taxon is scored erroneously as 'unknown' in more recent matrices.

In contrast to other eutriconodontans, *Spinolestes* (Martin et al. 2015) and the possible 'amphilestid' *Juchilestes* (Gao et al. 2010) are scored as having an enclosed pterygoparoccipital foramen. Based on the images presented we cannot verify or falsify the condition of the pterygoparoccipital foramen in *Spinolestes*. Martin et al. (2015) scored *Spinolestes* as possessing a gap between the lateral flange and crista parotica and in other eutriconodontans (i.e., *Astroconodon*, *Priacodon*, *Trioracodon*, and *Repenomamus*) the gap is equivalent with the pterygoparoccipital notch and as such we assume that a laterally open pterygoparoccipital notch is present in *Spinolestes*. The scoring of Gao et al. (2010: char. 332) for the pterygoparoccipital foramen as enclosed in the petrosal in *Juchilestes* might have been an error. Gao et al. (2010) noted that the "channel for the superior ramus of the stapedial artery [which is typically considered homologous to the pterygoparoccipital foramen/notch] is incompletely preserved and represented by a notch" (p. 241).

The fossa lateral to the crista parotica has been identified either as the fossa incudis or more broadly the epitympanic recess (Wible and Hopson 1993; Rougier et al. 1996; Meng

et al. 2011). In extant mammals the fossa incudis is usually the deepest area of the epitympanic recess that houses the crus breve of the incus. The epitympanic recess is the space that accommodates the articulation between the malleus and incus; it is typically shallower and broader than the fossa incudis and is positioned dorsal or dorsomedial to the tympanic membrane (MacPhee 1981; Meng et al. 2011). While the part of the epitympanic recess that forms the fossa incudis is better defined by bony landmarks, the epitympanic recess is less well delineated by bony morphology in basal mammaliaforms. The epitympanic recess (or a defined fossa for the epitympanic recess) is absent in the basal mammaliaforms *Morganucodon*, *Megazostrodon*, and *Haldanodon* as well as in the monotreme *Ornithorhynchus* (Zeller 1989; Wible and Hopson, 1995: fig. 4, Rougier et al. 1996: char. 25, Luo et al. 2002; Ruf et al. 2013). It was originally also scored as absent in the eutriconodontans *Trioracodon*, *Priacodon*, *Astroconodon* (i.e., the 'Cloverly triconodonts') and *Gobiconodon* (Rougier et al. 1996: char. 25, Luo et al. 2002: char. 216). In contrast, a large depression on the petrosal, squamosal or both is present in multituberculates, spalacotherioids, and basal cladotherians (e.g., Wible 1990, 2003; Fox and Meng 1997; Wible and Rougier 2000; Luo et al. 2002, 2012; Wible et al. 2009).

In *Astroconodon* the fossa incudis is deep and well defined by the crista parotica medially and two vertically oriented crests along the posterior and anterior margin. The lateral border is poorly preserved in the specimens at hand, but we suspect that the squamosal may have contributed to the lateral border of the fossa incudis. The boundaries of the epitympanic recess that contains the fossa incudis are less distinct in *Astroconodon*, but it appears to be a relatively large and deep fossa between the crista parotica medially and the squamosal laterally. In *Trioracodon*, Wible and Hopson (1993: fig. 5.3B) labeled the deep fossa lateral to the crista parotica 'fossa incudis'. The fossa was previously described by Kermack (1963: p. 88) as the "lateral pit" "to the left of this [anterior] part of the paroccipital process." The fossa incudis of *Trioracodon* has a medial border formed by the crista parotica, and an anterior and lateral border that is formed by a distinct crest. The crest is indicated in the reconstruction by Wible and Hopson (1993: fig. 5.3B) as a continuation of the lateral flange and is visible on the specimen (Kermack 1963: fig. 3). The fossa in *Trioracodon* resembles the morphology of that of the Cisco Mammal Quarry petrosals OMNH 80536 and OMNH 80537 (Davis et al. 2021: figs. 3 and 4), with the deepest portion of the epitympanic recess forming the fossa incudis immediately posterior to the proposed position of the incudomalleolar articulation.

Rougier et al. (1996) also described a deeply concave fossa incudis on the petrosal in *Priacodon*, with well-developed borders medially (crista parotica) and posteriorly (paroccipital process) but only a weakly developed anteromedial ridge and lacking a lateral margin. Rougier et al. (1996) did not specify whether the lack of a lateral border is due to preservation alone. The posterior border of the fossa incudis is broken away, along with most of the paroccipital process in the holotype of *Priacodon fruitaensis* (LACM 120451). Although the squamosal is not preserved in *Priacodon*, Rougier et al. (1996) were able to identify the facet for the squamosal on the petrosal, which extends almost to the anterior border of the fossa incudis. Rougier et al. (1996) entertained the possibility that the squamosal contributed to the missing lateral margin of the fossa incudis in life, a condition assumed or present in a variety of early mammaliaforms (Rougier et al. 1992, 1996; Rougier and Wible 2006). Despite the earlier scorings by Rougier et al. (1996) and Luo et al. (2002), an epitympanic recess is present in *Astroconodon*. We suspect that an epitympanic recess may have also been present in *Trioracodon* and *Priacodon* and that the specimens are just too incomplete to fully assess the morphology. In fact, Wible and Hopson (1993: p. 58) already indicated that "an epitympanic recess without a squamosal wall is identified as a synapomorphy of […] triconodontids […] by Luo (1988)", suggesting that it is not only present but a uniting characteristic of Triconodontidae. Whether the squamosal contributed to the epitympanic recess is not possible to assess in the incomplete specimens of *Trioracodon* and *Priacodon* and the area is impacted by poor preservation in *Astroconodon* but we suspect that the squamosal indeed contributed to the epitympanic recess in at least *Astroconodon*.

Aside from triconodontids an epitympanic recess has been identified in the eutriconodontans *Repenomamus* and *Liaoconodon*. In *Liaoconodon* the epitympanic recess is a shallow depression medial to the glenoid fossa that is bordered by the petrosal and squamosal (Meng et al. 2011). Meng et al. (2011: fig. 2), however, did not delineate the fossa incudis specifically in *Liaoconodon*. Based on the new evidence from *Liaoconodon,* Meng et al. (2011: Supplementary Material p. 17) also revised the original identification of the fossa incudis in *Repenomamus,* stating that the recess in *Repenomamus* is "shallow and large enough to accommodate not only the crus breve of the incus but also the malleo-incudal articulation" and thus should be called the epitympanic recess. An epitympanic recess is also scored as present lateral to the crista parotica in *Spinolestes*, but without a contribution from the squamosal (Martin et al. 2015: char. 385, 346). The figures in Martin et al. (2015) are not detailed enough to identify the outline or depth of the epitympanic recess or fossa incudis. It appears that an epitympanic recess was present in at least some eutriconodontans (i.e., *Astroconodon*, *Liaoconodon*, *Repenomamus*, *Spinolestes*) but that the size and bony elements contributing to the fossa may have varied in eutriconodontans. The epitympanic recess is deep with a clearly defined fossa incudis

in *Astroconodon* (at least a deep fossa incudis was also present in *Trioracodon* and *Priacodon*) whereas the epitympanic recess is shallow and the fossa incudis is indistinct in *Liaoconodon* and *Repenomamus*. The squamosal appears to have contributed to the lateral border of the epitympanic recess in *Astroconodon*, *Liaoconodon*, *Repenomamus* but not in *Spinolestes*.

Astroconodon has a pronounced crest lateral to the lateral trough that extends posteriorly from the foramen of the inferior ramus of the stapedial artery to terminate anterior to the crista parotica. Most of the crest is formed by the lateral flange of the petrosal, but the alisphenoid contributes to the anterior-most aspect of it. The lateral flange is an extension of the ventral edge of the anterior lamina of the petrosal and it is present in Mesozoic mammaliaforms that have an anterior lamina (Rougier and Wible 2006). In non-mammaliaform cynodonts and several basal mammaliaforms the alisphenoid (=epipterygoid) and the pterygoid (in basal cynodonts) also contribute to the formation of the crest through the quadrate ramus (Luo and Crompton 1994; Rougier and Wible 2006). Extant mammals lack a discrete quadrate ramus of the alisphenoid, possibly related to the exclusive function of the incus (=quadrate) as an auditory ossicle that no longer transmits mechanical forces (Rougier and Wible 2006) or to changes to the neurocranium in association with a relatively much larger brain (Rowe 1996; Rowe et al. 2011).

In *Astroconodon* the lateral flange of the petrosal forms much of the crest and extends up to the level of the foramina in the anterior part of the lateral trough. The quadrate ramus of the alisphenoid is present but confined to the anterior most portion of the crest. Congruent with our interpretation, Crompton and Luo (1993: fig. 4.12C) labeled the crest in *Astroconodon* at the level of the mid-point of the promontorium as lateral flange and did not indicate any other element contributing to the crest. Rougier et al. (1996: fig. 5D) labeled the character state of a ventrally directed lateral flange in *Astroconodon* even more anteriorly along the crest at the level of the anterior foramina in the lateral trough. The crest is incomplete in *Priacodon* but what is preserved is identified as lateral flange in Rougier et al. (1996). Wible and Hopson (1993: fig. 5.3B) also indicated the lateral flange in *Trioracodon* roughly at the level of the mid-point of the promontorium, similar to the position in Crompton and Luo (1993: fig. 4.12C) in *Astroconodon* and did not label any other element contributing to the crest. In the gobiconodontid *Repenomamus* the lateral flange is labeled at the very anterior aspect of the lateral trough in Meng et al. (2003: fig. 3).

In contrast to those reconstructions, Crompton and Sun (1985: fig. 7A) labeled the same crest lateral to the lateral trough (roughly at the level of the mid-point of the promontorium) 'quadrate ramus of the epipterygoid' [alisphenoid]. Neither Crompton and Luo (1993) nor Crompton and Sun (1985) nor Rougier et al. (1996: fig. 5D) indicate a suture between the alisphenoid and petrosal or a separation between the quadrate ramus of the alisphenoid and lateral flange of the petrosal in the reconstructions of *Astroconodon*; in fact, neither did Rougier et al. (1996: fig. 5E) nor Wible and Hopson (1993: fig. 5.3B) for *Trioracodon*. The same crest is simply labeled 'lateral flange' in Crompton and Luo (1993: fig. 4.12C), Rougier et al. (1996: fig. 5D, E), Wible and Hopson (1993: fig. 5.3B) and 'quadrate ramus of the epipterygoid' (=alisphenoid) in Crompton and Sun (1985: fig. 7A). Rougier et al. (1996: p. 9) more explicitly addressed the issue of the composition of the crest in *Priacodon* stating that the "ventral surface of the lateral flange (to the extent preserved) shows no facet for articulation with the quadrate ramus of the alisphenoid. However, the presence of a well-developed quadrate ramus underlying the missing anterior part of the lateral flange cannot be excluded." Similarly, the crest is not preserved past the anterior extent of the promontorium in *Trioracodon* and it is possible that the alisphenoid contributed to the extension of the crest more anteriorly, like it does in *Astroconodon*.

Presence of the quadrate ramus of the alisphenoid has also been addressed in several matrices (most of which do not include *Astroconodon*). The only matrix that includes *Astroconodon* (Rougier et al. 1996: char. 37) scored the contact between the petrosal and quadrate ramus of the alisphenoid as 'unknown' for *Astroconodon* and *Priacodon* and as 'small or absent' in *Trioracodon*. Luo et al. (2002: char. 206) scored the quadrate ramus of the alisphenoid as 'absent' in *Trioracodon* and *Gobiconodon* and 'unknown' in *Priacodon*. Hu (2006: char. 244) was the first to score the quadrate ramus as 'present' in *Repenomamus*, suggesting that additional unpublished specimens might show the separation between the quadrate ramus and lateral flange in greater detail than those published by Wang et al. (2001) and Meng et al. (2003), both of which labeled the crest in question as 'lateral flange'. In more recent matrices (Martin et al. 2015: char. 373; Mao et al. 2020: char. 383) *Repenomamus* and *Gobiconodon* are both scored as having a quadrate ramus and *Priacodon* and *Trioracodon* are left as 'unknown'. It is possible that a quadrate ramus of the alisphenoid is more common in Eutriconodonta. *Astroconodon* provides the first direct evidence of the quadrate ramus of the alisphenoid in Triconodontidae and it is possible that more complete specimens of *Priacodon* and *Trioracodon* reveal a similar morphology.

The placement of the tympanic opening of the prootic canal exhibits some variation among Triconodontidae. In *Astroconodon* the tympanic opening of the prootic canal is lateral to the crista parotica and anterior to the anteroposterior level of the fenestra vestibuli, whereas the foramen is medial to the crista parotica and at the level of the fenestra

vestibuli in *Trioracodon* (Kermack 1963; Wible and Hopson 1993: fig. 5.3B) and *Priacodon* (Rougier et al. 1996). The position of the tympanic opening of the prootic canal is rarely indicated or discussed in other eutriconodontans, the only other example is *Repenomamus* where it is indicated lateral to the fenestra vestibuli and medial to the pterygoparoccipital notch (Wang et al. 2001: fig. 2). The tympanic opening of the prootic canal appears to be in a more anterior position in concert with the longer crista parotica in *Astroconodon* compared with that in *Trioracodon*, *Priacodon* and *Repenomamus*.

As in most other eutriconodontans the geniculate ganglion of *Astroconodon* would have been ventrally enclosed by a bony floor of the petrosal to form the cavum supracochleare. A bony floor to the cavum supracochleare is scored as 'present' in *Gobiconodon*, *Repenomamus*, *Jeholodens*, *Trioracodon*, *Priacodon*, and *Juchilestes* (Rougier et al. 1996: char. 33; Hu 2006: char. 240; Mao et al. 2020: char. 378). Rougier et al. (1996: char. 33) originally scored the floor of the geniculate ganglion as ventrally open in *Priacodon*. Luo et al. (2002: char. 203) revised the scoring to 'presence of a bony floor that encloses the geniculate ganglion' in *Priacodon*, and this scoring has been accepted in subsequent iteration and revision of this matrix. G.W. Rougier (pers. comm. 04/2023) noted that the cavum supracochleare was only partially covercd by the slender bridge between the previously identified "primary facial foramen" and the tympanic opening of the prootic canal in *Priacodon*.

In *Astroconodon* the hyomandibular branch of the facial nerve would have left the cavum supracochleare through the secondary facial foramen medial to the crista parotica and immediately posterior to the transverse ridge. Crompton and Luo (1993) previously identified the secondary facial foramen in this location and our CT data and virtual reconstructions support this placement. In contrast, Wible and Hopson (1993: fig. 5.3B) and Kermack (1963) labeled the foramen posterior to the transverse ridge and medial to the crista parotica as the tympanic opening of the prootic canal in *Trioracodon*. This reconstructed position for the tympanic opening of the prootic canal in *Trioracodon* thus appears to be in a similar position to the secondary facial foramen in *Astroconodon* (Fig. 4). Furthermore, neither Kermack (1963) nor Wible and Hopson (1993) were able to identify the secondary facial foramen in *Trioracodon*. Kermack (1963: p. 89) speculated on the position of the secondary facial foramen in *Trioracodon*, but concluded that the course of the facial nerve "must be left with some uncertainty". Wible and Hopson (1993: fig. 5.3B) included a tentative position of the secondary facial foramen anterior to the transverse ridge but stated in the figure caption that the area is damaged, and that the position for the secondary facial foramen was modeled after the reconstructions of *Astroconodon* (the 'Cloverly triconodontid') by Crompton and Sun (1985). Crompton and Sun (1985: fig. 7A) indicated a foramen both posterior and anterior to the transverse ridge in the lateral trough of *Astroconodon*, but did not label either. We could not find a large foramen immediately anterior to the transverse ridge in the lateral trough in any of the *Astroconodon* specimens that we examined, and we do not believe that a foramen similar in size to the secondary facial foramen existed (see also Crompton and Luo 1993: fig. 4.12C). In *Priacodon*, the hyomandibular branch of the facial nerve likely exited through the tympanic opening of the prootic canal with the prootic sinus (pers. comm. G.W. Rougier 04/2023). The greater petrosal nerve would have left through the previously identified "primary facial foramen". In other words, in *Priacodon* the hyomandibular branch of the facial nerve exited posterior to the transverse ridge that forms the partial floor of the cavum supracochleare and the hiatus Fallopii is placed anterior to the transverse ridge (Fig. 4c). A similar arrangement might also be assumed for *Trioracodon*. The morphology of *Priacodon* and *Trioracodon* is basically identical with a slender ridge passing from the fenestra vestibuli laterally to the lateral flange separating a large tympanic opening of the prootic canal from a smaller hiatus Fallopii. Passage of the hyomandibular branch of the facial nerve through the tympanic opening of the prootic canal in *Trioracodon* would explain why neither Kermack (1963) nor Wible and Hopson (1993) were able to identify the secondary facial foramen. The general passage of the facial nerve would thus be conserved in triconodontids, with a floored or partially floored cavum supracochleare and the hyomandibular branch of the facial nerve exiting posterior to the transverse ridge. The facial nerve would have passed with the prootic sinus in *Trioracodon* and *Priacodon* but would have been separated from the prootic sinus in *Astroconodon*. Although we could not identify the position of the hiatus Fallopii in *Astroconodon*, we assume that the greater petrosal nerve likely followed a similar pattern to that of *Priacodon* and *Trioracodon* and opened into the lateral trough anterior to the transverse ridge at about mid-level (anteroposteriorly) of the promontorium.

In *Astroconodon* there seems to be a connection between the cavum supracochleare (which enclosed the geniculate ganglion) and the cavum epiptericum (which enclosed the trigeminal ganglion) through the fenestra semilunaris. A fenestra semilunaris between the space for the geniculate and trigeminal ganglions persists in some Mesozoic mammaliaforms, including *Morganucodon*, *Haldanodon*, paulchoffatiids, *Vincelestes* and metatherians (Kermack et al. 1981; Rougier et al. 1992; Crompton and Luo 1993; Lillegraven and Hahn 1993; Wible and Hopson 1993; Ruf et al. 2013). Rougier et al. (1996: char. 40) scored the geniculate ganglion as separate from the cavum epiptericum in *Trioracodon*, *Priacodon*, and *Astroconodon* (the 'Cloverly triconodonts'). The CT data considered here, however, do

not appear to support this interpretation for *Astroconodon*. Alternatively, it is possible that the wall between the two spaces was very thin and is simply not preserved in the specimens considered here.

Vasculature

Three-dimensional reconstructions and or detailed descriptions of the venous system surrounding the cochlear canal are limited in Eutriconodonta. *Astroconodon* represents only the second virtual rendering of these vessels after *Priacodon* (Harper and Rougier 2019).

Both *Astroconodon* and *Priacodon* have a large canal or canals for the inferior petrosal sinus that pass along the medial aspect of the cochlear canal. Several canals cross the cochlear canal dorsally and ventrally to connect the canals for the inferior petrosal sinus and prootic sinus. The vascular canals crossing the cochlear canal are highly variable in *Astroconodon*, but some patterns can be discerned. On the dorsal surface there are one or two canals for the posterior epicochlear sinus but no canals for the anterior epicochlear sinus, mirroring the pattern in *Priacodon*. The anterior epicochlear sinus was particularly well developed into a dense network of canals in the Early Cretaceous Teete petrosals (Schultz et al. 2022a), one of the possible haramiyidan petrosal (PIN 5087/69) from Berezovsk (Schultz et al. 2022b), and the zhangheotheriid *Origolestes* (Mao et al. 2020: fig. S8D). In contrast, one or few anterior epicochlear sinus canals are present in *Morganucodon*, the docodontan *Borealestes* (Panciroli et al. 2019), and the possible haramiyidan petrosals PIN 5087/37 and PIN 5087/70 from Berezovsk (Schultz et al. 2022b). The posterior epicochlear sinus canal seems to be less variable, with most of the taxa and specimens mentioned above exhibiting a single canal for the posterior epicochlear sinus.

The hypocochlear sinuses on the ventral surfaces of the cochlear canal were particularly variable in *Astroconodon* and even differed between sides in the same individual, ranging from a single canal to a network of small canals that is limited to the basal portion of the cochlear canal. *Priacodon* falls within that range, with two hypocochlear sinus canals. A network of canals that is limited to the basal portion of the cochlear canal is also present in the zhangheotheriid *Origolestes* (Mao et al. 2020: fig. S8C). In contrast, in more basal mammaliaforms the hypocochlear sinus is formed by a dense network of canals, the circumpromontorial plexus. From the circumpromontorial plexus several small canals connect to the internal aspect of the cochlear canal along the base of the secondary lamina. This is the case in *Morganucodon* (Hoffmann et al. 2018), the docodontan *Borealestes* (Panciroli et al. 2019) and the possible haramiyidans and docodontan petrosals from Berezovsk (Schultz et al. 2022b). Interestingly, several small vascular canals pass within the base of the secondary osseous lamina in *Astroconodon* and *Priacodon* in the same position as the openings of the circumpromontorial plexus of basal mammaliaforms. There are no apparent connections to the cochlear canal itself, although it is possible that such canals are too small to be resolved in the available CT scans of *Astroconodon*. The same is true for *Priacodon*. Harper and Rougier (2019: p. 28) noted that the specimen shows 'no intersection between the circumpromontorial venous plexus with the cochlear endocast." In *Astroconodon* and *Priacodon* the secondary osseous lamina canals pass from the hypocochlear sinus canals to merge with the canal for the inferior petrosal sinus at the apex of the cochlear canal. The connection to the inferior petrosal sinus is less well preserved in *Astroconodon*, but it is clearly present in *Priacodon*. A similar vascular canal along the base of the secondary lamina is also present in the stem therian Höövör petrosals (Harper and Rougier 2019) and seems to be present in the zhangheotheriid *Origolestes* but the view presented in Mao et al. (2020: fig. S8C) does not allow for a definite identification. The eutriconodontans appear to represent an intermediate step between the extensive circumpromontorial plexus in basal mammaliaforms and the modiolar venous system of therians (Axelsson 1974; Harper and Rougier 2019).

In *Astroconodon* and *Priacodon* (as well as in the other Mesozoic mammaliaforms for which the vascular canals are known) the canals for the hypo- and epicochlear sinuses connect the inferior petrosal canal medially with the prootic canal laterally. Small conduits of the prootic canal are present in *Astroconodon* that open into the lateral trough just anterior to the fenestra vestibuli. Similar small vascular canals in the lateral trough have been noted in *Trioracodon* and *Priacodon*. A neurovascular foramen anterior to the fenestra vestibuli has been previously described by Kermack (1963) in *Trioracodon* and was also noted by Wible and Hopson (1993: fig. 5.3B). Rougier et al. (1996) further described "a tiny opening with a narrow sulcus" anterior to the fenestra vestibuli (labeled "foramen in promontorium") in *Priacodon* and recognized its correspondence with the vascular canal in *Trioracodon* identified by Kermack (1963: fig. 3).

Inner ear

One salient feature of the inner ear in *Astroconodon* and other triconodontids is the straightness of the cochlear canal. Simpson (1928: p. 86) first recognized that the cochlear canal in *Triconodon* is "almost straight", a condition that he referred to as "altogether unique among mammals and even more reptile-like than that seen in *Echidna*." In addition to *Triconodon*, a nearly straight cochlear canal is known for *Astroconodon* and *Priacodon*. The finger-like promontoria in

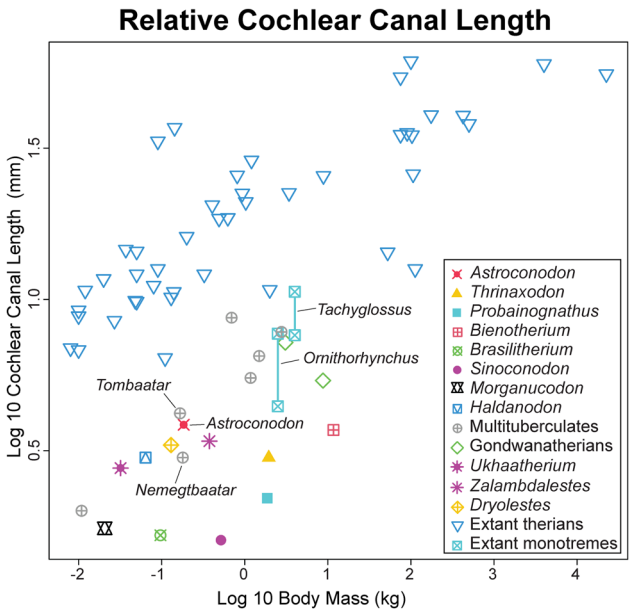

Fig. 5 Relationship between cochlear canal length and body mass in 46 extant and 20 extinct cynodonts, including *Astroconodon*. Values for most taxa follow Kirk et al. (2014: table 2) and Hoffmann and Kirk (2020). Cochlear canal length measurements were added for *Astroconodon* (3.85 mm; the mean of the right ear of MCZ 19973 and the left ear of MCZ 19974; Table 1) and *Taeniolabis* (7.8 mm; Krause et al. 2021). Estimated body mass values for *Astroconodon* (184 g) and *Taeniolabis* (2.769 kg) were derived from measurements of cranial length (*Astroconodon*: 43 mm, Table 1; *Taeniolabis*: 95.8 mm, Krause et al. 2021) using the equation $\log^{10}$body mass = ($\log^{10}$cranial length × 3.3832431)—6.261168 (Krause et al. 2020). Values for *Adalatherium* and *Vintana* are the maximum cochlear canal length and mean body mass estimates presented in Hoffmann and Kirk (2020). Values for extant monotremes (*Ornithorhynchus*, *Tachyglossus*) include total cochlear canal length (upper symbol; including lagena) and length of basilar membrane (lower symbol; excluding lagena)

other eutriconodontans (*Trioracodon, Repenomamus, Gobiconodon, Juchilestes*) suggest an equally straight cochlear canal for the whole clade. Comparably straight cochlear canals are rare among Mesozoic mammaliaforms and outside of Eutriconodonta are only known in the zhangheotheriids *Origolestes* (Mao et al. 2020: fig. S8) and *Zhangheotherium* (Luo et al. 2016: fig. 6.9). The cochlear canal is slightly curved in morganucodontans (Hoffmann et al. 2018), docodontans (Ruf et al. 2013; Panciroli et al. 2019), monotremes, the gondwanatherian *Vintana* (Hoffmann et al. 2014), and multituberculates (see discussion of cochlear canal shape in Krause et al. 2021). In contrast, the cochlear canal is coiled greater than 210 degrees in the gondwanatherian *Adalatherium* (Hoffmann and Kirk 2020) and in basal cladotherians (Rougier et al. 1992; Ruf et al. 2009; Luo et al. 2011, 2012; Harper and Rougier 2019). Accordingly, Harper and Rougier (2019) suggested that a straight cochlear canal might be a common feature at the base of Theriimorpha (i.e., therians and all extinct taxa closer to therians than to monotremes; Rowe 1993). This interpretation depends on the position of Eutriconodonta within Mammalia. If eutriconodontans are more basal than multituberculates and/or allotherians (e.g., as in Zhou et al. 2019 and Mao et al. 2020), then this topology might favor an independent origin of the straight cochlear canal in Zhangheotheria and Eutriconodonta.

Astroconodon and *Priacodon* show a lack of apical inflation of the cochlear canal, which may indicate that the lagenar macula was absent. The lagenar macula is often assumed to be present if the apex of the cochlear canal is inflated or a separate canal for the lagenar nerve is preserved. Based on one or both of those criteria a lagenar macula is assumed to have been present in the basal mammaliaform *Morganucodon*, the docodontans *Haldanodon* and *Borealestes*, the gondwanatherian *Adalatherium*, and the Berezovsk petrosals tentatively assigned to docodontans or haramiyidans (Ruf et al. 2013; Panciroli et al. 2019; Hoffmann and Kirk 2020; Schultz et al. 2022b). A slight apical inflation of the cochlear canal is also present in some but not all multituberculates (Fox and Meng 1997; Ladevèze et al. 2010; Schultz and Martin 2015; Weil and Tomida 2017; Csiki-Sava et al. 2018; Krause et al. 2021), which could indicate variation in the presence of a lagenar macula within Multituberculata or at least variation in the osteological correlates for the lagenar macula. By contrast, the tapering of the cochlear canal apex and presumptive absence of the lagenar macula in eutriconodontans may represent an independent loss of the lagena, as already suggested for the gondwanatherian *Vintana* (Hoffmann et al. 2014; Hoffmann and Kirk 2020), some multituberculates (Hurum 1998), and cladotherians (e.g., Luo et al. 2016).

The inferred lack of a lagenar macula in eutriconodontans has important implications for understanding the relationship between the lengths of the cochlear canal and cochlear duct in this clade. At about 8.4% of cranial length, the relative length of the cochlear canal in *Astroconodon* is broadly similar to a range of Mesozoic mammaliaforms including the gondwanatherian *Adalatherium* (8.6%), the docodontan *Haldanodon* (8.8–9.6%), and some multituberculates (e.g., *Tombaatar*, 9.5%; *Taeniolabis*, 8.1–9.1%) (Lillegraven and Krusat 1991; Ladevèze et al. 2010; Ruf et al. 2013; Hoffmann and Kirk 2020; Krause et al. 2021). These values are derived compared with more basal Mesozoic cynodonts such as *Probainognathus* (2.6%), *Sinoconodon* (2.7%), and *Morganucodon* (5.7–6.3%) (Luo et al. 1995), which have shorter cochlear canals relative to cranial length. Although some caution is required because both MCZ 19973 and MCZ 19974 were young individuals, these data suggest that the cochlear duct of *Astroconodon* is increased in relative length compared with the ancestral conditions for both Cynodontia and Mammaliaformes. This conclusion is reinforced by the fact that *Adalatherium*, *Haldanodon*, *Tombaatar*, and *Taeniolabis* are all interpreted as possessing

a lagenar macula that occupied the cochlear apex (Ladevèze et al. 2010; Ruf et al. 2013; Hoffmann and Kirk 2020; Krause et al. 2021). Accordingly, if we are correct in our inference that *Astroconodon* lacked a lagenar macula, then presumably its cochlear duct would have been even longer relative to cranial length than in Mesozoic taxa with comparable cochlear canal lengths that retained a lagenar macula. Nevertheless, the relative length of the cochlear duct in *Astroconodon* would have been markedly less than that observed in extant therians. This relationship is illustrated in Fig. 5, which plots cochlear canal length relative to observed or estimated body mass in a range of extant and fossil cynodonts. In this comparison, *Astroconodon* plots closest to the dryolestoid *Dryolestes*, the multituberculates *Tombaatar* and *Nemegtbaatar*, and the eutherian *Zalambdalestes*. The cochlear canal of *Astroconodon* is considerably longer than that of more basal Mesozoic cynodonts of similar body size (e.g., *Brasilitherium* and *Sinoconodon*) but substantially shorter than those of extant therians of similar body size (e.g., *Arvicola*, *Ctenomys*, and *Monodelphis*). Among the fossil taxa that compare most favorably with *Astroconodon* in Fig. 5, *Tombaatar* has been suggested to retain a lagenar macula (Ladevèze et al. 2010) while the lagenar macula is described as absent in *Nemegtbaatar* (Hurum 1998). Accordingly, the elevated position of *Tombaatar* on the y-axis relative to both *Astroconodon* and *Nemegtbaatar* in Fig. 5 may be expected if cochlear canal length in *Tombaatar* reflects the combined lengths of the cochlear duct and lagenar macula (as in extant monotremes) rather than the length of the cochlear duct alone (as in extant therians and as inferred for *Astroconodon*).

In total, these observations suggest that the length of the cochlear duct in *Astroconodon* was derived in being relatively long compared with many Mesozoic cynodonts, but was nevertheless much shorter than in extant therians. By the same token, the relative length of the cochlear canal in *Astroconodon* is not substantially shorter than that observed for the Cretaceous eutherians *Zalambdalestes* and *Ukhaatherium* (Fig. 5). These data favor the conclusion that the relative length of the cochlear canal was broadly similar in Eutriconodonta and basal Theria, and that the evolution of additional cochlear elongation in extant marsupials and placentals (Fig. 5) probably occurred in parallel. Although elongation of the cochlear duct in extant mammals may be generally related to an expansion of high frequency hearing abilities (e.g., Meng and Fox 1995; Kirk et al. 2014; Hoffmann and Kirk 2020), the precise implications of the unique cochlear anatomy observed in *Astroconodon* are not entirely clear due to a lack of extant taxa with comparable morphology. Perhaps the closest living analogues are extant monotremes, which also have shorter cochlear canals and cochlear ducts than extant therians (Fig. 5), lack a primary osseous lamina, and exhibit a variably present base of the secondary osseous lamina (Schultz et al. 2017). In both *Tachyglossus* and *Ornithorhynchus*, this morphology is associated with an expansion of high frequency hearing abilities to include frequencies less than 20 kHz but still well beyond those detectable by most extant non-mammalian tetrapods (Vater et al. 2004; Kirk et al. 2014). Accordingly, it seems likely that the high frequency hearing abilities of both eutriconodonts and basal therians were expanded compared with the ancestral cynodont and mammaliaform conditions. The potential functional consequences of having a relatively straight (e.g., as in eutriconodonts) or coiled cochlear duct (e.g., as in therians, *Dryolestes*, and *Adalatherium*) are currently unknown. Aside from allowing the cochlear duct to increase in length, Meng and Fox (1995) speculated that coiling of the cochlear duct minimize differences in length among the cochlear nerve fibers and may thereby minimize difference in nerve impulse conduction time between the apical and basal part of the hearing membrane. Based on mechanical modeling Manoussaki et al. (2008) put forth a different hypothesis that coiling might enhance low-frequency hearing. Their models suggested that a strongly coiled cochlear canal allows concentration of travelling wave energy along the innermost, apical turns, thereby increasing sensitivity to low frequencies. Harper and Rougier (2019) suggested that under this model the straight cochlear morphology as seen in *Priacodon* and the stem therian Höövöer petrosals in comparison to the gently curved cochlear canals of other early mammaliaforms may be seen as a modification to de-emphasize detection of lower-frequency sounds. However, Manoussaki et al. (2008) only looked a selected sample of extant placentals with cochlear turns greater than 1.75, so whether their model is applicable to extinct mammaliaforms with straight or slightly curved cochlear canals is uncertain.

Another feature used to estimate hearing frequencies in early mammaliaforms is the ossification of the primary and secondary lamina (e.g., Meng and Fox 1995; Fox and Meng 1997; Kirk et al. 2014; Luo et al. 2016). In therians the presence of osseous laminae may stiffen the basilar membrane and therefore lead to an upward shift in the range of resonant frequencies represented across the basilar membrane (Wever et al. 1971; Fleischer 1976; Ketten 1992; Kirk et al. 2014; Luo and Manley 2020). *Astroconodon* preserves a substantial base of a secondary osseous lamina that extends along the complete length of the cochlear canal. A similarly extensive base of the secondary osseous lamina is also present in *Priacodon* but has been scored as 'absent' in *Repenomamus*, *Gobiconodon*, *Liaoconodon*, *Jeholodens*, and *Juchilestes* (Gao et al. 2010: char. 309; Mao et al. 2020: char. 367). However, inner ear morphology has not been studied in-depth in any of those scored taxa and we suspect that at least some could in fact have a base of the secondary osseous lamina similar to that of *Astroconodon* and *Priacodon*. A similarly deep and long base of the secondary osseous lamina is also present in the zhangheotheriid *Origolestes* (Mao et al. 2020: fig. S8E). In addition to zhangheotheriids

and eutriconodontans, a shorter base of the secondary osseous lamina, is known in the gondwanatherians *Adalatherium* and *Vintana* (Hoffmann et al. 2014; Hoffmann and Kirk 2020) and in cladotherians (Luo et al. 2016). In the gondwanatherian *Adalatherium* the secondary osseous lamina base extends about half the length of the cochlear canal, whereas it is much shorter in cladotherians. The secondary osseous lamina ends slightly anterior to the fenestra cochleae in *Henkelotherium* and *Dryolestes* (Ruf et al. 2009; Luo et al. 2012), after the first turn in *Vincelestes* (Rougier 1993), and extends to between 25–50% of total cochlear canal length in some Cretaceous eutherians (Ekdale 2009, 2013; Ekdale and Rowe 2011).

Interestingly, eutriconodontans and zhangheotheriids lack a primary osseous lamina. Lack of a primary osseous lamina but variable presence of the base of the secondary osseous lamina is also seen in monotremes (Schultz et al. 2017). Within mammals the primary osseous lamina first appeared (likely independently) in gondwanatherians and cladotherians (Hoffmann et al. 2014; Hoffmann and Kirk 2020). *Astroconodon* adds to the growing evidence that the base of the secondary lamina ossified before the primary lamina. While the primary osseous lamina is universally present in therians and its function in supporting the basilar membrane is well established (Echteler et al. 1994), how the development of a base of the secondary osseous lamina without a primary osseous lamina relates to the structural support of the hearing membrane remains unclear (Manley 2018; Harper and Rougier 2019; Luo and Manley 2020). We speculate that basal cladotherians (Meng and Fox 1995; Ruf et al. 2009; Ekdale and Rowe 2011; Luo et al. 2011, 2012; Ekdale 2013) that have relatively short cochlear ducts but possess both a primary and secondary osseous laminae may have had high frequency hearing abilities that were further expanded compared with eutriconodonts, which lack a primary osseous lamina.

Priacodon and *Astroconodon* both lack a secondary crus commune between the lateral and posterior semicircular canal. A secondary crus commune is present in extant monotremes (Denker 1901) and in many Mesozoic mammaliaforms, including the docodontan *Haldanodon* (Ruf et al. 2013), the Berezovsk petrosals (Schultz et al. 2022b), the multituberculate *Tombaatar* (Ladevèze et al. 2010), the gondwanatherian *Vintana* (Hoffmann et al. 2014), the zhangheotheriid *Origolestes* (Mao et al. 2020), the dryolestidans *Dryolestes* and *Henkelotherium* (Ruf et al. 2009; Luo et al. 2012) and several basal eutherians and metatherians (Meng and Fox 1995; Ekdale 2009, 2013; Ekdale and Rowe 2011). In contrast, a secondary crus commune is, in addition to the eutriconodontans, only absent in some multituberculates and most extant therians (Meng and Wyss 1995; Hurum 1998; Ekdale 2013; Luo et al. 2016; Krause et al. 2021).

Conclusion

The inner ear and associated neurovascular structures of *Astroconodon* represent only the second three-dimensional reconstruction of eutriconodontan ear morphology. Eutriconodonta is one of the most widespread Mesozoic mammaliaform clades, ranging from the Early/Middle Jurassic to the Late Cretaceous and being known from most continents (except Australia and Antarctica). Eutriconodonta includes the largest and first carnivorous Mesozoic mammaliaforms and are recognized from some exceptionally well-preserved skeletons (e.g., Hu et al. 2005; Hu 2006; Luo et al. 2007; Gaetano and Rougier 2011; Meng et al. 2011; Martin et al. 2015). Despite this widespread occurrence, the inner ear morphology of the clade has received relatively little attention. This fact is even more surprising given that some of the earliest descriptions of Mesozoic mammaliaform petrosal anatomy is based on triconodontid eutriconodontans (Simpson 1928; Kermack 1963).

The inner ear of *Astroconodon* and other eutriconodontans exhibit a nearly straight cochlear canal and a long and deep base of the secondary osseous lamina paired with the possible absence of a lagenar macula. This combination of features suggests that *Astroconodon*, and eutriconodontans in general (Harper and Rougier 2019), might be taking a different route to increase hearing capabilities by increasing the length of the cochlear canal in a straight fashion rather than coiling the cochlear canal as is seen in contemporary stem therians and by stabilizing the hearing membrane through a particularly long secondary osseous lamina. In addition, at least triconodontids (if not all eutriconodontans) share the absence of an anterior epicochlear sinus and the presence of a hypocochlear sinus, posterior epicochlear sinus, and vascular canals that extend along the base of the secondary osseous lamina. This canal or set of canals in the base of the secondary osseous lamina differs from the extensive circumpromontorial plexus seen in more basal mammaliaforms.

Several inner ear features may link eutriconodontans to zhangheotheriid stem therians. Both groups are characterized by a marked straightness of the cochlear canal and a particularly long and deep base of the secondary osseous lamina. Occurrence of those features either represents an example of homoplasy in cochlear evolution or could support a phylogenetic position of Eutriconodonta closer to Trechnotheria and a common origin of those features in the stem therian lineage.

Supplementary information The online version contains supplementary material available at https://doi.org/10.1007/s10914-023-09673-5.

Acknowledgements We are grateful to A.W. Crompton and F.A. Jenkins, Jr. for access to the Cloverly triconodontid specimens; C. R. Schaff and W. Amaral for preparation of specimens; and M. Colbert and J. Maisano (University of Texas – Austin) for µCT imaging. We are grateful to J. R. Wible (Carnegie Museum of Natural History) for

sharing information on vasculature reconstructions; G. W. Rougier (University of Louisville) for detailed discussion on bony morphology and development; reviewers J. Meng (American Museum of Natural History) and G. W. Rougier for insightful comments that greatly improvement the manuscript; and editors J. A. Schultz and D. Croft for handling the manuscript.

Funding Partial support for this research was provided by National Science Foundation grants DEB-9870173 and FRES 1925896.

Data availability Surface files of the inner ear and associated neurovasculature are available on MorphoSource (https://www.morphosource.org/projects/000532321). The original tiff stacks are not publicly available due to ongoing work on the skull anatomy.

Declarations

Competing interest SH is an associate editor for the Journal of Mammalian Evolution but was not involved in the evaluation of this manuscript.

References

Astin TR (1986) Septarian crack formation in carbonate concretions from shales and mudstones. Clay Miner 21:617–631. https://doi.org/10.1180/claymin.1986.021.4.12

Axelsson A (1974) The vascular anatomy of the rhesus monkey cochlea. Acta Otolaryngol 77:381–392. https://doi.org/10.3109/00016487409124640

Brown DA, Sherriff BL, Sawicki JA, Sparling R (1999) Precipitation of iron minerals by a natural microbial consortium. Geochim Cosmochim Acta 63:2163–2169. https://doi.org/10.1016/S0016-7037(99)00188-X

Butler PM, Sigogneau-Russell D (2016) Diversity of triconodonts in the Middle Jurassic of Great Britain. Pal Pol 67:35–65.

Cifelli RL, Lipka TR, Schaff CR, Rowe TB (1999) First Early Cretaceous mammal from the eastern seaboard of the United States. J Vertebr Paleontol 19:99–203. https://doi.org/10.1080/02724634.1999.10011134

Cifelli RL, Madsen SK (1998) Triconodont mammals from the medial Cretaceous of Utah. J Vertebr Paleontol 18:403–411. https://doi.org/10.1080/02724634.1998.10011068

Cifelli RL, Wible JR, Jenkins FA Jr (1998) Triconodont mammals from the Cloverly Formation (Lower Cretaceous), Montana and Wyoming. J Vertebr Paleontol 18:237–24. https://doi.org/10.1080/02724634.1998.10011048

Clemens WA, Lillegraven JA, Lindsay EH, Simpson GG (1979) Where, when, and what – a survey of known Mesozoic mammal distribution. In: Lillegraven JA, Kielan-Jaworowska Z, Clemens WA (eds) Mesozoic Mammals: The First Two-Thirds of Mammalian History. University of California Press, Berkeley and Los Angeles, pp 7–58.

Csiki-Sava Z, Vremir M, Meng J, Brusatte SL, Norell MA (2018) Dome-headed, small-brained island mammal from the Late Cretaceous of Romania. Proc Natl Acad Sci USA 115:4857–4862. https://doi.org/10.1073/pnas.1801143115

Crompton AW, Luo Z-X (1993) Relationships of the Liassic mammals, *Sinoconodon*, *Morganucodon oehleri*, and *Dinnetherium*. In: Szalay FS, Novacek MJ, McKenna MC (eds) Mammal Phylogeny: Mesozoic Differentiation, Multituberculates, Monotremes, Early Therians, and Marsupials. Springer Verlag, New York, pp 30–44. https://doi.org/10.1007/978-1-4613-9249-1_4

Crompton AW, Sun A (1985) Cranial structure and relationships of the Liassic mammal *Sinoconodon*. Zool J Linn Soc 85:99–119. https://doi.org/10.1111/j.1096-3642.1985.tb01500.x

Davis BM, Cifelli RL, Rougier GW (2021) Mammalian petrosals from the Upper Jurassic Morrison Formation (Utah, USA) reveal non-canonical evolution of middle and inner ear characters. J Mamm Evol 28:1027–1049. https://doi.org/10.1007/s10914-021-09586-1

Denker A (1901) Zur Anatomie des Gehörorgans der Monotremata. Semon Zool. Forschungsreisen Austr 3:635–662

Echteler SM, Fay RR, Popper AN (1994) Structure of the mammalian cochlea. In: Fay RR, Popper AN (eds) Comparative Hearing: Mammals. Springer Verlag, New York, New York, pp 134–171

Ekdale EG (2009) Variation within the bony labyrinth of mammals. Dissertation, The University of Texas at Austin

Ekdale EG (2013) Comparative anatomy of the bony labyrinth (inner ear) of placental mammals. PLOS One 8:e66624. https://doi.org/10.1371/journal.pone.0066624

Ekdale EG, Rowe TB (2011) Morphology and variation within the bony labyrinth of zhelestids (Mammalia, Eutheria) and other therian mammals. J Vertebr Paleontol 31:658–675. https://doi.org/10.1080/02724634.2011.557284

Fleischer G (1976) Hearing in extinct cetaceans as determined by cochlear structure. J Paleontol 50:133–152

Fox RC (1969) Studies of Late Cretaceous vertebrates. III. A triconodont mammal from Alberta. Can J Zool 47:1253–1256. https://doi.org/10.1139/z69-196

Fox RC (1976) Additions to the mammalian local fauna from the upper Milk River Formation (Upper Cretaceous), Alberta. Can J Earth Sci 13:1105–1118

Fox RC, Meng J (1997) An X-radiographic and SEM study of the osseous inner ear of multituberculates and monotremes (Mammalia): implications for mammalian phylogeny and evolution of hearing. Zool J Linn Soc 121:249–291. https://doi.org/10.1111/j.1096-3642.1997.tb00339.x

Gaetano LC, Rougier GW (2011) New materials of *Argentoconodon fariasorum* (Mammaliaformes, Triconodontidae) from the Jurassic of Argentina and its bearing on triconodont phylogeny. J Vertebr Paleontol 31:829–843. https://doi.org/10.1080/02724634.2011.589877

Gao C-L, Wilson GP, Luo Z-X, Maga M, Meng Q, Wang X (2010) A new mammal skull from the Lower Cretaceous of China with implications for the evolution of obtuse-angled molars and 'amphilestid' eutriconodonts. Proc R Soc B 277:237–246. https://doi.org/10.1098/rspb.2009.1014

Goodrich ES. (1930) Studies on the Structure and Development of Vertebrates. Macmillan and Co., London.

Harper T, Rougier GW (2019) Petrosal morphology and cochlear function in Mesozoic stem therians. PLOS One 14:e0209457. https://doi.org/10.1371/journal.pone.0209457

Hoffmann S, Kirk EC (2020) Inner ear morphology of *Adalatherium hui* (Mammalia, Gondwanatheria) from the Late Cretaceous of Madagascar. In: Krause DW, Hoffmann S (eds) *Adalatherium hui* (Mammalia, Gondwanatheria) from the Late Cretaceous of Madagascar. Soc Vertebr Paleontol Mem 21. J Vertebr Paleontol 40(5, Suppl):67–80. https://doi.org/10.1080/02724634.2020.1800719

Hoffmann S, O'Connor PM, Kirk EC, Wible JR, Krause DW (2014) Endocranial and inner ear morphology of *Vintana sertichi* (Mammalia, Gondwanatheria) from the Late Cretaceous of Madagascar. In: Krause DW (ed) *Vintana sertichi* (Mammalia, Gondwanatheria) from the Late Cretaceous of Madagascar. Soc Vertebr Paleontol Mem 14. J Vertebr Paleontol 34(6, Suppl):110–136. https://doi.org/10.1080/02724634.2014.956878

Hoffmann S, Shahid R, Watanabe A, Gill P (2018) Large sampling from Early Jurassic fissure fillings reveals variation in cochlear canal shape in the basal mammaliaform *Morganucodon*. J Vertebr Paleontol, Progr Abstr:147

Hu Y (2006) Postcranial morphology of *Repenomamus* (Eutriconodonta, Mammalia): implications for the higher-level phylogeny of mammals. Dissertation, City University of New York

Hu Y, Meng J, Wang Y, Li C (2005) Large Mesozoic mammals fed on young dinosaurs. Nature 433:14–9152. https://doi.org/10.1038/nature03102

Hurum JH (1998) The inner ear of two Late Cretaceous multituberculate mammals, and its implications for multituberculate hearing. J Mammal Evol 5:65–93. https://doi.org/10.1023/A:1020571003901

Jenkins FA Jr, Crompton AW (1979) Triconodonta. In: Lillegraven JA, Kielan-Jaworowska Z, Clemens WA (eds) Mesozoic Mammals: The First Two-Thirds of Mammalian History. University of California Press, Berkeley, pp 74–90

Jenkins FA Jr, Schaff CR (1988) The Early Cretaceous mammal *Gobiconodon* (Mammalia, Triconodonta) from the Cloverly Formation in Montana. J Vertebr Paleontol 8:1–24. https://doi.org/10.1080/02724634.1988.10011681

Ji Q, Luo Z-X, Ji S-A (1999) A Chinese triconodont mammal and mosaic evolution of mammalian skeleton. Nature 398:326–330. https://doi.org/10.1038/18665

Kermack KA (1963) The cranial structure of the triconodonts. Philos Trans R Soc B Biol 246:83–103. https://doi.org/10.1098/rstb.1963.0002

Kermack KA, Mussett F, Rigney HW (1981) The skull of *Morganucodon*. Zool J Linn Soc 71:1–158. https://doi.org/10.1111/j.1096-3642.1981.tb01127.x

Ketten DR (1992) The marine mammal ear: specializations for aquatic audition and echolocation. In: Webster DB, Popper AN, Fay RR (eds) The Evolutionary Biology of Hearing. Springer, New York, pp 717–750

Kielan-Jaworowska Z, Cifelli RL, Luo Z-X (2004) Mammals from the Age of Dinosaurs: Origins, Evolution, and Structure. Columbia University Press, New York.

Kirk EC, Hoffmann S, Kemp AD, Krause DW, O'Connor PM (2014) Sensory Anatomy and Sensory Ecology of *Vintana Sertichi* (Mammalia, Gondwanatheria) from the Late Cretaceous of Madagascar. In: Krause DW (ed) *Vintana sertichi* (Mammalia, Gondwanatheria) from the Late Cretaceous of Madagascar. Soc Vertebr Paleontol Mem 14. J Vertebr Paleontol 34(6, Suppl):110–136. https://doi.org/10.1080/02724634.2014.963232

Krause DW, Hoffmann S, Hu Y, Wible JR, Rougier GW, Kirk EC, Groenke JR, Rogers RR, Rossie JB, Schultz JA, Evans AR (2020) Skeleton of a Cretaceous mammal from Madagascar reflects long-term insularity. Nature 581:421-427. https://doi.org/10.1038/s41586-020-2234-8

Krause DW, Hoffmann S, Lyson TR, Dougan LG, Petermann H, Tecza A, Chester SG, Miller IM (2021) New skull material of *Taeniolabis taoensis* (Multituberculata, Taeniolabididae) from the early Paleocene (Danian) of the Denver Basin, Colorado. J Mammal Evol. 28:1083–143. https://doi.org/10.1007/s10914-021-09584-3

Kusuhashi N, Hu Y, Wang Y, Hirasawa S, Matsuoka H (2009) New triconodontids (Mammalia) from the Lower Cretaceous Shahai and Fuxin formations, northeastern China. Geobios 42:765–781. https://doi.org/10.1016/j.geobios.2009.06.003.

Ladevèze S, de Muizon C, Colbert M, Smith T (2010) 3D computational imaging of the petrosal of a new multituberculate mammal from the Late Cretaceous of China and its paleobiologic inferences. Comptes Rendus Palevol 9:319–330. https://doi.org/10.1016/j.crpv.2010.07.008

Li C, Wang Y, Hu Y, Meng J (2003) A new species of *Gobiconodon* (Triconodonta, Mammalia) and its implication for the age of Jehol Biota. Chin Sci Bull 48:1129–1134. https://doi.org/10.1007/BF03185767

Li J, Wang Y, Wang Y, Li C (2001) A new family of primitive mammals from the Mesozoic of western Liaoning, China. Chin Sci Bull 46: 782–785. https://doi.org/10.1007/BF03187223

Lillegraven JA, Hahn G (1993) Evolutionary analysis of the middle and inner ear of Late Jurassic multituberculates. J Mammal Evol 1:47–74. https://doi.org/10.1007/BF01027599

Lillegraven JA, Krusat G (1991) Cranio-mandibular anatomy of *Haldanodon exspectatus* (Docodonta; Mammalia) from the Late Jurassic of Portugal and its implications to the evolution of mammalian characters. Contri Geol Univ Wash 28:39–138

Lucas SG, Luo Z-X (1993) *Adelobasileus* from the Upper Triassic of West Texas: the oldest mammal. J Vertebr Paleont 13:309–334. https://doi.org/10.1080/02724634.1993.10011512

Luo Z (1988) Two distinct patterns of apomorphous petrosal characters among major mammalian groups and their phylogenetic implications. J Vertebr Paleontol Suppl. 8:20A

Luo Z-X, Chen P, Li G, Chen M (2007) A new eutriconodont mammal and evolutionary development in early mammals. Nature 446:288–293. https://doi.org/10.1038/nature05627

Luo Z-X, Crompton AW (1994) Transformation of the quadrate (incus) through the transition from non-mammalian cynodonts to mammals. J Vertebr Paleontol 14:341–374. https://doi.org/10.1080/02724634.1994.10011564

Luo Z-X, Crompton AW, Lucas SG (1995) Evolutionary origins of the mammalian promontorium and cochlea. J Vertebr Paleontol 15:113–121. https://doi.org/10.1080/02724634.1995.10011211

Luo Z-X, Ekdale EG, Schultz JA (2016) Evolution of the middle and inner ears of mammaliaforms: the approach to mammals. In: Clack JA, Far RR, Popper AN (eds) Evolution of the Vertebrate Ear. Springer Handbook Aud Res, Cham, pp 139–174. https://doi.org/10.1007/978-3-319-46661-3_6

Luo Z-X, Ji Q, Wible JR, Yuan C-X (2003) An Early Cretaceous tribosphenic mammal and metatherian evolution. Science 302:1934–1939. https://doi.org/10.1126/science.1090718

Luo Z-X, Kielan-Jaworowska Z, Cifelli RL (2002) In quest for a phylogeny of Mesozoic mammals. Acta Palaeont Pol 47:1–78

Luo Z-X, Manley GA (2020) Origins and early evolution of mammalian ears and hearing function. In: Fritzsch B (ed) The Senses: A Comprehensive Reference. Elsevier, pp 207–252. https://doi.org/10.1016/B978-0-12-805408-6.00033-6

Luo Z-X, Martin T, Ruf I (2012) The petrosal and inner ear of the Late Jurassic cladotherian mammal *Dryolestes leiriensis* and implications for ear evolution in therian mammals. Zool J Linn Soc 166:433–463. https://doi.org/10.1111/j.1096-3642.2012.00852.x

Luo Z-X, Martin T, Ruf I, Schultz JA (2011) Fossil evidence on evolution of inner ear cochlea in Jurassic mammals. Proc R Soc Lond 278:28–34. https://doi.org/10.1098/rspb.2010.1148

MacPhee RDE (1981) Auditory regions of primates and eutherian insectivores: morphology, ontogeny and character analysis. Contrib Primat 18:1–282

Manoussaki D, Chadwick RS, Ketten DR, Arruda J, Dimitriadis EK, O'Malley JT (2008). The influence of cochlear shape on low-frequency hearing. Proc Natl Acad Sci USA 105:6162–6166. https://doi.org/10.1073/pnas.0710037105

Manley GA (2018) The foundations of high-frequency hearing in early mammals. J Mamm Evol 25:155–163

Mao F, Hu Y, Li C, Wang Y, Chase MH, Smith AK, Meng J (2020) Integrated hearing and chewing modules decoupled in a Cretaceous stem therian mammal. Science 367:305–308. https://doi.org/10.1126/science.aay9220

Mao F, Zhang C, Liu C, Meng J. (2021) Fossoriality and evolutionary development in two Cretaceous mammaliamorphs. Nature 592:577–582. https://doi.org/10.1038/s41586-021-03433-2

Marsh OC (1887) American Jurassic Mammals. Am J Sci 23:81–92

Martin T, Averianov AO (2010) Mammals from the Middle Jurassic Balabansai Formation of the Fergana Depression, Kyrgyzstan. J Vertebr Paleontol 30:855–871. https://doi.org/10.1080/02724631003758045

Martin T, Marugan-Lobon J, Vullo R, Martin-Abad H, Luo Z-X, Buscalioni AD (2015) A Cretaceous eutriconodont and integument evolution in early mammals. Nature 526:380–384. https://doi.org/10.1038/nature14905

Martinez-Ruiz F, Jroundi F, Paytan A, Guerra-Tschuschke I, del Mar Abad M, González-Muñoz MT (2018) Barium bioaccumulation by bacterial biofilms and implications for Ba cycling and use of Ba proxies. Nat Commun 9:1619. https://doi.org/10.1038/s41467-018-04069-z

Meng J, Fox RC (1995) Osseous inner ear structures and hearing in early marsupials and placentals. Zool J Linn Soc 115:47–71. https://doi.org/10.1111/j.1096-3642.1995.tb02323.x

Meng J, Hu Y, Wang Y, Li C (2003) The ossified Meckel's cartilage and internal groove in Mesozoic mammaliaforms: implications to origin of the definitive mammalian middle ear. Zool J Linn Soc 138:431–448. https://doi.org/10.1046/j.1096-3642.2003.00064.x

Meng J, Hu Y, Wang Y, Wang X, Li C (2006) A Mesozoic gliding mammal from northeastern China. Nature 444:889–893. https://doi.org/10.1038/nature05234

Meng J, Wang Y, Li C (2011) Transitional mammalian middle ear from a new Cretaceous Jehol eutriconodont. Nature 472:181–185. https://doi.org/10.1038/nature09921

Meng J, Wyss AR (1995) Monotreme affinities and low-frequency hearing suggested by multituberculate ear. Nature 377:141–144. https://doi.org/10.1038/377141a0

Panciroli E, Luo Z-X, Schultz JA (2019) Morphology of the petrosal and stapes of *Borealestes* (Mammaliaformes, Docodonta) from the Middle Jurassic of Skye, Scotland. Pap Palaeontol 5:139–156. https://doi.org/10.1002/spp2.1233

Patterson B (1951) Early Cretaceous mammals from northern Texas. Am J Sci 249:31–46. https://doi.org/10.2475/ajs.249.1.31

Rougier GW (1993) *Vincelestes neuquenianus* Bonaparte (Mammalia, Theria) un Primitivo Mamífero del Cretácico Inferior de la Cuenca Neuquina. Dissertation, Universidad Nacional de Buenos Aires

Rougier GW, Forasiepi AM, Martinelli AG (2021) Mesozoic Mammals from South America and Their Forerunners. Springer Cham, Switzerland. https://doi.org/10.1007/978-3-030-63862-7

Rougier GW, Hopson JA, Wible JR (1992) Reconstruction of the cranial vessels in the Early Cretaceous mammal *Vincelestes neuquenianus*: implications for the evolution of the mammalian cranial system. J Vertebr Paleontol 12:188–216. https://doi.org/10.1080/02724634.1992.10011449

Rougier GW, Martinelli AG, Forasiepi AM, Novacek MJ (2007) New Jurassic mammals from Patagonia, Argentina: a reappraisal of australosphenidan morphology and interrelationships. Am Mus Novit 3566:1–54. http://hdl.handle.net/2246/5857

Rougier GW, Wible JR (2006) Major changes in the ear region and basicranium of early mammals. In: Carrano MT, Gaudin TJ, Blob RW, Wible JR (eds) Amniote Paleobiology: Phylogenetic and Functional Perspectives on the Evolution of Mammals, Birds, and Reptiles. University of Chicago Press, Chicago, pp 269–311

Rougier GW, Wible JR, Hopson JA (1996) Basicranial anatomy of *Priacodon fruitaensis* (Triconodontidae, Mammalia) from the Late Jurassic of Colorado, and a reappraisal of mammaliaform interrelationships. Am Mus Novit 3183:1–38. http://hdl.handle.net/2246/3639

Rowe TB (1993) Phylogenetic systematics and the early history of mammals. In: Szalay FS, Novacek MJ, McKenna MC (eds) Mammal Phylogeny, Volume 1—Mesozoic Differentiation, Multituberculates, Monotremes, Early Therians, and Marsupials. Springer Verlag, New York, pp 129–145. https://doi.org/10.1007/978-1-4613-9249-1_10

Rowe TB (1996) Brain heterochrony and evolution of the mammalian middle ear. In: Ghiselin M, Pinna G (eds) New Perspectives on the History of Life: Essays on Systematic Biology as Historical Narrative. Calif Acad Sci Mem 20, San Francisco, pp 71–96

Rowe TB, Macrini TE, Luo Z-X (2011) Fossil evidence on origin of the mammalian brain. Science 332:955–957. https://www.science.org/doi/10.1126/science.1203117

Ruf I, Luo Z-X, Martin T (2013) Reinvestigation of the basicranium of *Haldanodon exspectatus* (Mammaliaformes, Docodonta). J Vertebr Paleontol 33:382–400. https://doi.org/10.1080/02724634.2013.722575

Ruf I, Luo Z-X, Martin T, Wible JR (2009) Petrosal anatomy and inner ear structures of the Late Jurassic *Henkelotherium* (Mammalia, Cladotheria, Dryolestoidea): insight into the early evolution of the ear region in cladotherian mammals. J Anat 214:679–693. https://doi.org/10.1111/j.1469-7580.2009.01059.x

Schultz JA, Luo Z-X, Zeller U (2017) Inner ear labyrinth anatomy of monotremes and implications for mammalian inner ear evolution. J Morphol 278:236–263. https://doi.org/10.1002/jmor.20632

Schultz JA, Martin T (2015) The inner and middle ear of Jurassic paulchoffatiid multituberculates. J Vertebr Paleontol, Progr Abstr: 210

Schultz JA, Ruf I, Averianov AO, Schellhorn R, Lopatin AV, Martin T (2022b). Jurassic mammaliaform petrosals from Western Siberia (Russia) and implications for early mammalian inner-ear anatomy. Zool J Linn Soc 196:1175–1200. https://doi.org/10.1093/zoolinnean/zlab096

Schultz JA, Schellhorn R, Skutschas PP, Vitenko DD, Kolchanov VV, Grigoriev DV, Kuzmin IT, Kolosov PN, Lopatin AV, Averianov AO, Martin T (2022a) Mammalian petrosal from the Lower Cretaceous high paleo-latitude Teete locality (Yakutia, Eastern Russia). Vertebr Zool 72:159–168. https://doi.org/10.3897/vz.72.e78479

Simpson GG (1928) A Catalogue of the Mesozoic Mammalia in the Geological Department of the British Museum. British Museum (Natural History), London

Simpson GG (1929) American Mesozoic Mammalia. Mem Peabody Mus 3:1–235

Vater M, Meng J, Fox RC (2004) Hearing organ evolution and specialization: early and later mammals. In: Manley GA, Fay RR, Popper AN (eds) Evolution of the Vertebrate Auditory System. Springer Verlag, New York, pp 256–288. https://doi.org/10.1007/978-1-4419-8957-4_9

Wang Y, Hu Y, Meng J, Li C (2001) An ossified Meckel's cartilage in two Cretaceous mammals and the origin of the mammalian middle ear. Science 294:357–361. https://doi.org/10.1126/science.1063830.

Weil A, Tomida Y (2017) Inner ear of the cimolodontan multituberculate *Meniscoessus robustus* supports functional interpretation and a novel phylogenetic hypothesis. FASEB J 31(S1). https://doi.org/10.1096/fasebj.31.1_supplement.243.2

Wever EG, McCormick JG, Palin J, Ridgeway SH (1971) Cochlea of the dolphin, *Tursiops truncatus*: the basilar membrane. Proc Natl Acad Sci USA 68:2708–2711. https://doi.org/10.1073/pnas.68.11.270

Wible JR (1990) Petrosals of Late Cretaceous marsupials from North America, and a cladistic analysis of the petrosal in therian mammals. J Vertebr Paleontol 10:183–205. https://doi.org/10.1080/02724634.1990.10011807

Wible JR (2003) On the cranial osteology of the short-tailed opossum *Monodelphis brevicaudata* (Didelphidae, Marsupialia). Ann Carnegie Mus 72:137–202

Wible JR (1991) Origin of Mammalia: the craniodental evidence reexamined. J Vertebr Paleontol 11:1–28. https://doi.org/10.1080/02724634.1991.10011372

Wible JR, Hopson JA (1993) Basicranial evidence for early mammal phylogeny. In: Szalay FS, Novacek MJ, McKenna MC (eds) Mammal Phylogeny, Volume 1—Mesozoic Differentiation, Multituberculates, Monotremes, Early Therians, and Marsupials. Springer Verlag, New York, pp 45–62. https://doi.org/10.1007/978-1-4613-9249-1_5

Wible JR, Hopson JA (1995) Homologies of the prootic canal in mammals and non-mammalian cynodonts. J Vertebr Paleontol 15:331–356. https://doi.org/10.1080/02724634.1995.10011233

Wible JR, Rougier GW (2000) Cranial anatomy of *Kryptobaatar dashzevegi* (Mammalia, Multituberculata), and its bearing on the evolution of mammalian characters. Bull Am Mus Nat Hist 247:1–124. http://hdl.handle.net/2246/1594

Wible JR, Rougier GW, Novacek MJ, Asher RJ (2009) The eutherian mammal *Maelestes gobiensis* from the Late Cretaceous of Mongolia and the phylogeny of Cretaceous Eutheria. Bull Am Mus Nat Hist 327:1–123. http://hdl.handle.net/2246/6001

Zeller U (1989) Die Enwicklung und Morphologie des Schädels von *Ornithorhynchus anatinus* (Mammalia: Prototheria: Monotremata). Abhandlungen Senck Naturf Ges 545:1–188

Zeller U (1993) Ontogenetic evidence for cranial homologies in monotremes and therians, with special reference to *Ornithorhynchus*. In: Szalay FS, Novacek MJ, McKenna MC (eds) Mammal Phylogeny, Volume 1—Mesozoic Differentiation, Multituberculates, Monotremes, Early Therians, and Marsupials. Springer Verlag, New York, pp 95–107. https://link.springer.com/chapter/10.1007/978-1-4613-9249-1_8

Zhou C-F, Bhullar B-AS, Neander AI, Martin T, Luo Z-X (2019) New Jurassic mammaliaform sheds light on early evolution of mammal-like hyoid bones. Science 365:276–279. https://doi.org/10.1126/science.aau9345